The Journal of Immunology

A Transgenic Line That Reports CSF1R Protein Expression Provides a Definitive Marker for the Mouse Mononuclear Phagocyte System

Kathleen Grabert, Anuj Sehgal, Katharine M. Irvine, Evi Wollscheid-Lengeling, Derya D. Ozdemir, Jennifer Stables, Garry A. Luke, Martin D. Ryan, Antony Adamson, Neil E. Humphreys, Cheyenne J. Sandrock, Rocio Rojo, Veera A. Verkasalo, Werner Mueller, Peter Hohenstein, Allison R. Pettit, Clare Pridans and David A. Hume

J Immunol 2020; 205:3154-3166; Prepublished online 2 November 2020;
doi: 10.4049/jimmunol.2000835
http://www.jimmunol.org/content/205/11/3154

The Journal of Immunology is published twice each month by
The American Association of Immunologists, Inc.,
1451 Rockville Pike, Suite 650, Rockville, MD 20852

Print ISSN: 0022-1767 Online ISSN: 1550-6606.

A Transgenic Line That Reports CSF1R Protein Expression Provides a Definitive Marker for the Mouse Mononuclear Phagocyte System

Kathleen Grabert,*[,1] Anuj Sehgal,[†,1] Katharine M. Irvine,[†,1] Evi Wollscheid-Lengeling,* Derya D. Ozdemir,* Jennifer Stables,[†] Garry A. Luke,[‡] Martin D. Ryan,[‡] Antony Adamson,[§] Neil E. Humphreys,[§] Cheyenne J. Sandrock,[†] Rocio Rojo,[¶] Veera A. Verkasalo,[‖] Werner Mueller,[§] Peter Hohenstein,* Allison R. Pettit,[†] Clare Pridans,[‖,2] and David A. Hume[†,2]

The proliferation, differentiation, and survival of cells of the mononuclear phagocyte system (MPS; progenitors, monocytes, macrophages, and classical dendritic cells) are controlled by signals from the M-CSF receptor (CSF1R). Cells of the MPS lineage have been identified using numerous surface markers and transgenic reporters, but none is both universal and lineage restricted. In this article, we report the development and characterization of a CSF1R reporter mouse. A FusionRed (FRed) cassette was inserted in-frame with the C terminus of CSF1R, separated by a T2A-cleavable linker. The insertion had no effect of CSF1R expression or function. CSF1R-FRed was expressed in monocytes and macrophages and absent from granulocytes and lymphocytes. In bone marrow, CSF1R-FRed was absent in lineage-negative hematopoietic stem cells, arguing against a direct role for CSF1R in myeloid lineage commitment. It was highly expressed in marrow monocytes and common myeloid progenitors but significantly lower in granulocyte-macrophage progenitors. In sections of bone marrow, CSF1R-FRed was also detected in osteoclasts, CD169$^+$ resident macrophages, and, consistent with previous mRNA analysis, in megakaryocytes. In lymphoid tissues, CSF1R-FRed highlighted diverse MPS populations, including classical dendritic cells. Whole mount imaging of nonlymphoid tissues in mice with combined CSF1R-FRed/*Csf1r*-EGFP confirmed the restriction of CSF1R expression to MPS cells. The two markers highlight the remarkable abundance and regular distribution of tissue MPS cells, including novel macrophage populations within tendon and skeletal muscle and underlying the mesothelial/serosal/capsular surfaces of every major organ. The CSF1R-FRed mouse provides a novel reporter with exquisite specificity for cells of the MPS. ***The Journal of Immunology*****, 2020, 205: 3154–3166.**

The mononuclear phagocyte system (MPS) is a family of cells with related function and gene expression profiles, including progenitors, monocytes, tissue macrophages, and classical dendritic cells (cDC) (1). The proliferation, differentiation, and survival of most tissue macrophages depend upon signals from the M-CSF receptor (CSF1R). Homozygous recessive mutations in the receptor in mice, rats, and humans lead to loss of tissue macrophages and osteoclasts and pleiotropic developmental abnormalities in many organ systems (reviewed in Ref. 2). *Csf1r* mRNA is expressed by all resident tissue macrophages (3). The transcriptional regulation of the *Csf1r* gene has been studied extensively as a model of macrophage differentiation (4). Deletion of a conserved enhancer in the first intron (Fms intronic regulatory element, FIRE) leads to selective loss of *Csf1r*

*The Roslin Institute, University of Edinburgh, Easter Bush, Midlothian EH259RG, United Kingdom; [†]Mater Research Institute–University of Queensland, Translational Research Institute, Woolloongabba, Brisbane, Queensland 4102, Australia; [‡]School of Biology, University of St Andrews, North Haugh, St Andrews KY16 9ST, United Kingdom; [§]Faculty of Biology, Medicine and Health, School of Biological Sciences, Manchester M13 9PT, United Kingdom; [¶]Escuela de Medicina y Ciencias de la Salud, Tecnologico de Monterrey, 64710 Monterrey, Mexico; and [‖]Centre for Inflammation Research, University of Edinburgh, Little France, Edinburgh EH16 4TJ, United Kingdom

[1]K.G., A.S., and K.M.I. contributed equally.

[2]C.P. and D.A.H. are joint senior authors.

ORCIDs: 0000-0002-5628-9400 (K.G.); 0000-0002-5210-1730 (A.S.); 0000-0002-6716-1605 (K.M.I.); 0000-0001-6020-3297 (G.A.L.); 0000-0002-0012-0614 (M.D.R.); 0000-0002-5408-0013 (A.A.); 0000-0003-3210-4093 (N.E.H.); 0000-0002-4111-8393 (C.J.S.); 0000-0001-9686-3377 (R.R.); 0000-0002-9524-8919 (V.A.V.); 0000-0002-1297-9725 (W.M.); 0000-0001-8548-4734 (P.H.); 0000-0003-4707-7892 (A.R.P.); 0000-0001-9423-557X (C.P.); 0000-0002-2615-1478 (D.A.H.).

Received for publication July 20, 2020. Accepted for publication September 23, 2020.

This work was supported by UK Research and Innovation Medical Research Council (MRC) Grant MR/M019969/1 and by Australian National Health and Medical Research Council Grant GNT1163981 to D.A.H. D.A.H., K.M.I., and A.R.P. receive core support from The Mater Research Foundation. R.R. was supported by a doctoral scholarship (application number 314413, file number 21889) granted by the Centro de Investigación Científica y de Educación Superior de Ensenada, "Nuevo Leon—I2T2, Mexico" Baja California. P.H. was supported by UK Research and Innovation Biotechnology and Biological Sciences Research Council Grant BB/P013732/1. D.D.O. was supported by MRC Grant MR/M010341/1. We acknowledge support from the Microscopy and Cytometry facilities of the Translational Research Institute (TRI). TRI is supported by the Australian Government.

Address correspondence and reprint requests to Prof. David A. Hume, Mater Research Institute–University of Queensland, Translational Research Institute, 37 Kent Street, Woolloongabba, Brisbane, QLD 4102, Australia. E-mail address: david.hume@uq.edu.au

The online version of this article contains supplemental material.

Abbreviations used in this article: BM, bone marrow; BMDM, BM-derived macrophage; cDC, classical dendritic cell; CMP, common myeloid progenitor; DC, dendritic cell; ESC, embryonic stem cell; ESDM, ESC-derived macrophage; FRed, FusionRed; GMP, granulocyte-macrophage progenitor; HSC, hematopoietic stem cell; LN, lymph node; MEP, megakaryocyte-erythroid progenitor; MPS, mononuclear phagocyte system; MZ, marginal zone; RFP, red fluorescent protein; sgRNA, single-stranded guide RNA; WT, wild-type.

expression in tissue macrophage populations, including microglia in the brain (5). Transgenic reporters containing FIRE have been generated in mice (6, 7), rats (8), chickens (9, 10), and sheep (11) and in each species highlight the location and abundance of macrophage populations in every organ. However, there are caveats to the utility and interpretation of these *Csf1r* reporters. First, based on the phenotype of the $Csf1r^{\Delta FIRE/\Delta FIRE}$ mice, we identified regulatory elements outside of the transgene construct so that the absence of reporter gene detection in particular cells may be difficult to interpret (5). In the chick, we found that Kupffer cells expressed *Csf1r* mRNA and protein but did not express the *Csf1r*-mApple reporter transgene (12). Conversely, mouse and human granulocytes expressed *Csf1r* mRNA but did lack protein expression (13), and the *Csf1r* promoter also has detectable activity in B lymphocytes, which share expression of the transcriptional regulator PU.1 (14, 15). Accordingly, the *Csf1r* reporter transgenes in mouse, rat, and chicken were detectable in both granulocytes and B cells. In many tissues this is not a major issue; the macrophages have a characteristic location and stellate morphology (1, 16). But in lymphoid tissues, and mucosal surfaces and inflammatory sites, it would be desirable to separate these cell types.

There have been a number of reports on expression of CSF1R in nonhematopoietic cells, including neurons and neuronal progenitors in the brain and epithelial cells in the gut and kidney (17–19). In each case, the conclusion depends upon immunolocalization with poorly characterized polyclonal Abs or conditional reporter transgenes and was not supported by subsequent analyses (2). In the brain, the mouse *Csf1r*-EGFP reporter transgene and the protein detected by anti-CD115 Ab were expressed exclusively in microglia (20, 21). A further argument against functional expression of CSF1R in nonhematopoietic cells follows from the complete rescue of the pleiotropic impacts of *Csf1r* knockouts in mice (22) by postnatal adoptive transfer of wild-type (WT) bone marrow (BM) cells.

By contrast to surface markers such as F4/80, CD11b/c, CD163, CD68, CD169, CD64, CD206, CX3CR1, LYVE1, and MHC class II, which are expressed independently by subsets of tissue MPS cells (3, 16), CSF1R is a potential universal marker for cells of the MPS. There are available mAbs against the mouse CSF1R protein (CD115). Two different Abs have been described that block CSF1 binding to the mouse receptor and can deplete tissue macrophages (23, 24). Anti-CD115 Abs can detect cell surface expression on at least some myeloid progenitors in the BM (25) and on isolated blood monocytes (7) and can compete for binding of labeled CSF1 protein to tissue macrophages in vivo (6). However, CSF1R protein is not readily detected on most tissue macrophages by immunohistochemistry using monoclonal anti-CD115. The lack of detection is most likely a consequence of competition with endogenous ligand (the available Abs compete for CSF1 binding) and the downregulation of the receptor from the cell surface by ligand. CSF1 is internalized by receptor-mediated endocytosis, and both receptor and ligand are degraded (26). Accordingly, signaling requires continuous synthesis of new receptors. The surface receptor is also subject to rapid proteolytic cleavage in response to signals that activate macrophages (27, 28), and it is likely cleaved from the surface directly or indirectly during tissue disaggregation to isolate macrophages. All cell isolation procedures lead to activation of inflammatory genes in macrophages (3).

cDC were originally defined based on an apparent unique ability to present Ag to naive T cells. Class II MHC^+ migratory monocytes, monocyte-derived cells, and subsets of resident tissue macrophages also possess active Ag presentation activity (29–31). cDC and monocytes share a committed progenitor in the BM that expresses CSF1R (32). cDC have been classified separately from macrophages in different tissues and contexts based on the lack of certain surface markers, including CD64 (Fcgr1) and MERTK (33). One subset of mouse cDC, termed cDC2, shares many markers with monocytes and macrophages, including high expression of *Csf1r* mRNA and *Csf1r* reporter transgenes (3, 6, 34). cDC retain expression of the growth factor receptor FLT3, which is coexpressed with CSF1R on progenitors (25), and lymphoid tissue cDC are depleted in FLT3 or FT3L knockouts. However, CSF1R signaling can partly rescue the impacts of *Flt3* null mutation on lymphoid tissue cDC numbers (35), and CSF1 treatment can expand their numbers in the spleen (34). By contrast, cDC2 in nonlymphoid tissues depend upon CSF1R (36, 37), and all cells in nonlymphoid tissues expressing the *Csf1r* reporter transgene were completely depleted by anti-CSF1R Ab (23). We were therefore interested in whether dendritic cells (DC) defined by current markers express CSF1R protein.

In this study, we aimed to overcome the rapid turnover of surface CSF1R and ectopic expression in promoter-based transgenics by integrating a reporter gene into the mouse *Csf1r* locus. Knock-in reporters, for example, in the *Cx3Cr1* (38) and *Ccr2* loci (39), have been widely used in the study of macrophage biology, but in each case the endogenous gene is knocked out. Although heterozygous mutation of *Csf1r* has no overt phenotypic impact in mouse, rat, or human, there is no dosage compensation (2). Given the central role of CSF1R in macrophage homeostasis, a knockout insertion is undesirable. One alternative is to insert a cassette including an internal ribosome re-entry site downstream of the stop codon. This approach was used to generate an *Ms4a3* locus reporter that tags cells derived from myeloid progenitors and apparently separated monocyte-derived cells from cDC in tissues (40). To target microglia, Ruan et al. (41) inserted a tdTomato reporter with a cleavable peptide linker between the coding sequence and 3′-untranslated region of the *Tmem119* locus. Masuda et al. (42) inserted the same reporter into the *Hexb* locus. In this study, we took a similar approach and inserted a FusionRed (FRed) cassette with cleavable linker in-frame into the 3′ end of the mouse *Csf1r* locus. Analysis of this novel line confirms that CSF1R protein expression is restricted to macrophages and their committed progenitors and provides a universal functional differentiation marker for cells of the MPS lineage, including DC. Imaging of this reporter gene provides a unique picture of the extent of the MPS in tissues.

Materials and Methods

Generation of Csf1r-*T2A-FRed mice*

We used CRISPR-Cas9 to generate CSF1R C-terminally tagged with a T2A-FRed reporter gene. The overall strategy is shown in Fig. 1. Two single-stranded guide RNA (sgRNA) targeting the STOP codon of *Csf1r* were selected using the Sanger WTSI Web site (http://www.sanger.ac.uk/htgt/wge/). Guides present elsewhere in the genome with mismatches of zero, one, or two were discounted, and mismatches of three were considered if predicted off targets were not exonic. sgRNA sequences (AACTACCAGTTCTGCTGAAG-*TGG* and ACTACCAGTTCTGCTGAAGT-*GGG*) were purchased as CRISPR RNA oligos, which were annealed with *trans*-activating CRISPR RNA (both oligos supplied; IDT, Coralville, IA) in sterile, RNase-free injection buffer (TrisHCl 1 mM, pH 7.5, EDTA 0.1 mM). A total of 2.5 μg CRISPR RNA was combined with 5 μg *trans*-activating CRISPR RNA, heated to 95°C, then allowed to slowly cool to room temperature.

For the donor repair template, we used the EASI-CRISPR long-ssDNA strategy (43), which comprised the FRed gene with cleavable T2A linker flanked by 136- and 139-nt homology arms. The long-ssDNA donor was generated using Biotinylated PCR from a dsDNA template, followed by binding to streptavidin beads and on-bead denaturation to remove the bottom strand of DNA. The top ssDNA was then cleaved off the column by

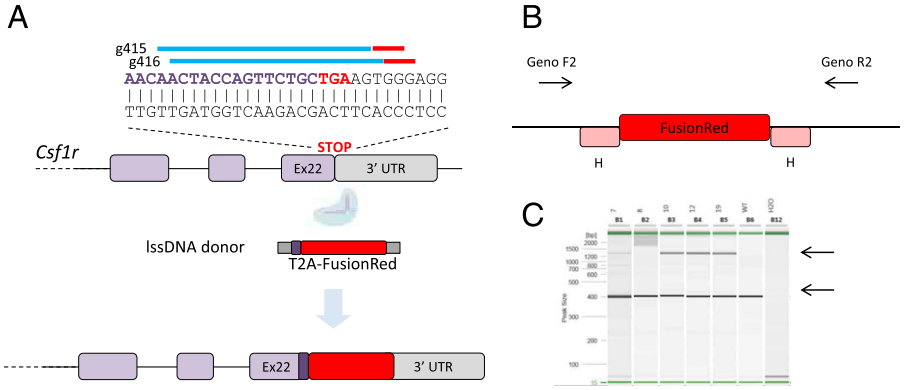

FIGURE 1. Design and generation of CSF1R-FRed transgene. (**A**) The schematic of the insertion of T2A-FRed into the mouse *Csf1r* locus with the guides and overall strategy as described in *Materials and Methods*. (**B**) The location of the PCR primers and (**C**) the detection of three independent founders with the desired insertion, which was sequence verified.

hybridizing a short oligo at the 5′ end to reform a KpnI restriction site and subjected to restriction digestion.

For embryo microinjection, the annealed sgRNA was complexed with Cas9 protein (New England Biolabs, Hitchin, U.K.) at room temperature for 10 min before addition of long-ssDNA donor (final concentrations: sgRNA 20 ng/μl, Cas9 protein 20 ng/μl, long-ssDNA 10 ng/μl). CRISPR reagents were directly microinjected into C57BL/6JOlaHsd zygote pronuclei using standard methods (44). Zygotes were cultured overnight, and the resulting two cell embryos surgically implanted into the oviduct of day 0.5 post-coitum pseudopregnant mice. Potential founder mice were screened by PCR, first using primers that flank the homology arms and sgRNA sites (Geno F2 ccaccccaggactatgctaa and Geno R2 ctagcactgtgagaacccca), a reaction which both amplifies the WT band (394 bp), any InDels that result from nonhomologous end joining activity and larger products (1153 bp) that would result from homology-dependent repair (Fig. 1). Pups with a larger band were reserved, the band was isolated and amplified again using high-fidelity Phusion polymerase (New England Biolabs), and gel was extracted and subcloned into pCRblunt (Invitrogen). Colonies were mini-prepared and Sanger sequenced with M13 forward and reverse primers. Pups showed perfect sequence integration after alignment of sequence traces to predicted knock-in sequence and bred with a WT C57BL/6JOlaHsd to confirm germline transmission and establish the colony. The founders were subsequently transferred to specific-pathogen-free facilities in Edinburgh and Brisbane by rederivation and crossed to the C57BL/6JCrl background.

Tissue collection for imaging and disaggregation for flow cytometry analysis

Peripheral blood (100 μl) was routinely collected into EDTA tubes by cardiac puncture following euthanasia. Blood was subjected to RBC lysis for 2 min in ACK lysis buffer (150 mM NH_4Cl, 10 mM $KHCO_3$, 0.1 mM EDTA, pH 7.4) and resuspended in flow cytometry buffer (PBS/2% FBS) for staining. Peritoneal cells were recovered by lavage with 10 ml of PBS. Following lavage, tissues of interest were removed for disaggregation and imaging. Tissues for imaging were stored in PBS on ice and imaged within 2 h.

Liver and brain tissues for disaggregation were finely chopped in digestion solution containing 1 mg/ml Collagenase IV, 0.5 mg/ml Dispase (Worthington), and 20 μg/ml DNAse1 (Roche) and placed on ice until further processing (~1 g of tissue/10 ml). Tissues in digestion solution were placed on a rocking platform at 37˚C for 45 min prior to mashing through a 70-μm filter (Falcon). For liver and brain, Percoll density gradient centrifugation was used to isolate the nonparenchymal fraction, as previously described (5, 6). Cell isolation from BM, spleen, and lymph node (LN) was carried out as described (45). A total of 5×10^6 cells were stained for flow cytometry analysis, and $1–2 \times 10^6$ cells were acquired for analysis.

Flow cytometry

Cell preparations were stained for 45 min on ice in 2.4.G2 hybridoma supernatant to block Fc receptor binding. Myeloid populations were stained using Ab mixtures (45) comprising combinations of CD45-BV421, F4/80-AF647, CD11b-BV510, CD115-BV605, Ly6G-BV785 or APC-Fire750, TIM4-PECy7, Ly6C-PB or BV785, B220-APCCy7 or BUV496, TER119-BUV395, and CD3-PE-Cy5 (BioLegend). Hematopoietic stem and progenitor cells were stained using a standard Ab mixture comprising of Lineage-BV785 (CD3-, CD45R-, CD41-, CD11b-, GR1-, and TER119-biotin followed by streptavidin-BV785), cKIT-APC, SCA-1-PE-Cy7, CD150-BV650, CD48-BV421, and CD115-BV605 (BioLegend). Myeloid and lymphoid progenitors were stained using an Ab mixture composed of Lineage-BV785 (CD3-, CD45R-, CD11b-, GR1- and TER119-biotin followed by streptavidin-BV785), c-KIT-APC, SCA-1-PE-Cy7, CD34-PerCP-Cy5.5, CD16/32-BV421, and FLT3-APC-Cy7. Cells were washed twice following staining and resuspended in flow cytometry buffer containing 7AAD (Life Technologies) or FVS700 (BD Bioscience) for acquisition using a Cytoflex (Beckman Coulter) or Fortessa (Becton Dickinson). Relevant single-color controls were used for compensation, and unstained and fluorescence-minus-one controls were used to confirm gating strategies. Flow cytometry data were analyzed using FlowJo 10 (Tree Star). Live single cells were identified for phenotypic analysis by excluding doublets (FSC-A > FSC-H), $7AAD^+$, or $FVS700^+$ dead cells and debris.

Confocal microscopy and immunofluorescence

All immunofluorescent images were acquired on the Olympus FV3000 microscope (Olympus) and FLUOVIEW software (Olympus). To prepare tissues for immunofluorescent staining, spleens, LN, livers, and lungs were snap frozen in liquid nitrogen, and bones were first fixed in 4% paraformaldehyde. Bones were then further decalcified in 14% EDTA over 3 wk with several changes before sucrose saturation in 15–30% sucrose gradient over 2 d. All tissues were then embedded in Optimal cutting temperature compound (ProSciTech) and cut at 5 μm thickness. FRed in the bones was stained using Rabbit anti–red fluorescent protein (RFP) Ab (ab62341; Abcam). Cell-specific staining for macrophage phenotypic markers was performed using a monoclonal rat anti-F4/80 (Abcam) or directly conjugated anti-CD169-AF488 or anti-CD68-AF647 (both BioLegend). B cells and T cells were detected using anti-B220-AF488 (BioLegend) and anti-CD3-AF647, respectively (BD Bioscience). Unconjugated primary Abs were detected with fluorescently labeled species appropriate secondary Abs, including goat anti-rabbit IgG Alexa Fluor 594 (Thermo Fisher Scientific) and goat anti-rat IgG Alexa Fluor 647 (Thermo Fisher Scientific). All sections of bone, spleen, LN, liver, lungs, and brain images were acquired with a ×200 magnification objective using the multiarea tile scan function. For direct imaging of wholemount tissues, tissues were left as undisturbed as possible for direct imaging through the tissue surface. For tissues with reduced laser penetration (such as spleen or kidney), tissues were trimmed to a relative thickness of 2 mm and imaged from the surface in. The Z-stack function of the software was used to acquire a greater depth of field. For wholemount imaging of small intestine, 1-mm pieces of small intestine were fixed for 1 h in BD Cytofix/Cytoperm buffer before staining with a rat anti-F4/80 monoclonal (Abcam). Secondary staining was performed using an anti-rat AF647 (Thermo Fisher Scientific), and B cells were stained using anti-B220-AF488 (BioLegend). CSF1R-FRed signal was acquired using the 561-diode laser, and *Csf1r*-EGFP or AF488 was acquired using the 488-diode laser, both on the FV3000 main combiner (FV31-MCOMB). For DAPI or AF647, signal was acquired using the 405- and 633-diode lasers, respectively, on the FV3000 main combiner (FV31-MCOMB).

Results

Development and validation of a strategy to generate a translational CSF1R reporter

To overcome the limitations of the current *Csf1r* reporter transgenes, we aimed to generate a transgene that would accurately mirror protein expression. The ideal outcome would place a reporter cassette in-frame with the CSF1R protein to generate a fusion protein that would mark the plasma membrane and allow

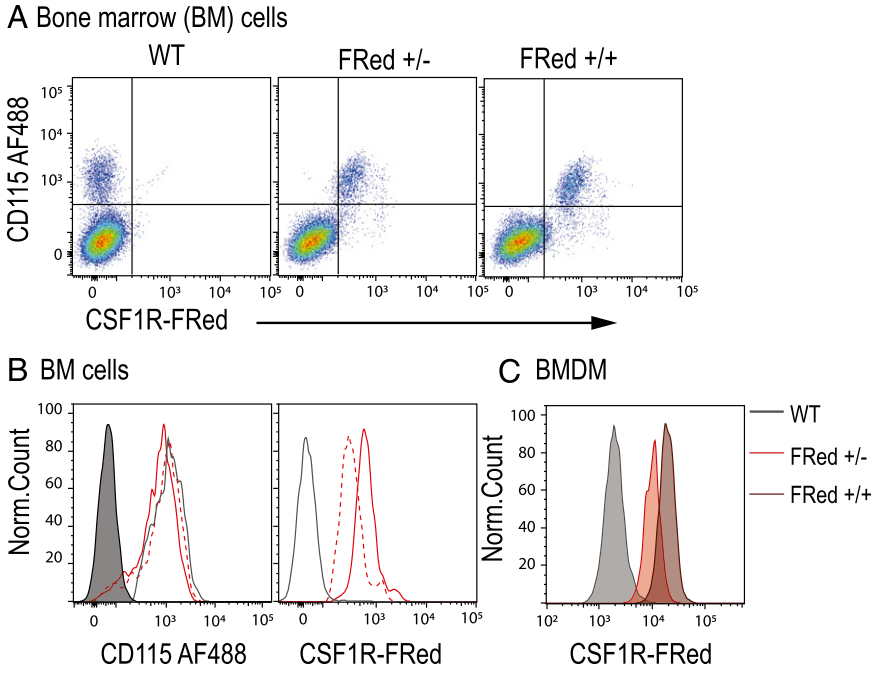

FIGURE 2. Expression of CSF1R-FRed in BM and BMDM. (**A**) The relationship between CSF1R-FRed and surface CSF1R (CD115) on unfractionated BM cells from adult mice in WT (C57BL/6 control), heterozygous (CSF1R-FRed$^{+/-}$), and homozygous CSF1R-FRed$^{+/+}$ mice. (**B**) Histograms of the same profiles, with fill profile WT, dotted line CSF1R-FRed$^{+/-}$, and filled line CSF1R-FRed$^{+/+}$. Note that the expression of the two markers is correlated and there is a right shift in FRed in the homozygote. (**C**) BMDM were grown from WT, CSF1R-FRed$^{+/-}$, and CSF1R-FRed$^{+/+}$ BM cells as described in *Materials and Methods*. The cells were harvested after 7 d and analyzed by flow cytometry.

analysis of intracellular trafficking. We previously expressed functional CSF1R from several species in transfected cells with a V5-His C-terminal tag (46, 47) and anticipated that it could be possible to create a CSF1R-RFP fusion. To enable double imaging with EGFP reporter lines, we chose FRed. This protein has been tested as a fusion partner in multiple applications and has the additional advantage of being resistant to photobleaching (48). A CSF1R-FRed fusion allele was generated by CRISPR-mediated recombination in embryonic stem cells (ESC), and expression was analyzed in ESC-derived macrophages (ESDM) as described previously (5). We confirmed the successful targeting of one allele in ESC, which did not prevent the generation of ESDM. However, there was no detectable FRed expression. As an alternative, we tested the insertion of a cleavable linker. For this purpose, we used the T2A peptide also used in the recent targeting of *Hexb* (42). T2A was originally identified in picornavirus (49) and enables the generation of multiple proteins from a single viral mRNA. The 2A oligopeptides mediate ribosomal skipping, which appears as "self-cleavage" with stoichiometric expression of two or more translation products. Self-cleaving peptide linkers have been used in multicistronic vectors in vitro (50) and in vivo (51, 52). FRed was absent from transfected ESC but was detected in ESDM by flow cytometry and direct imaging (data not shown). On this basis, we proceeded to generate CSF1R-FRed mice as outlined in Fig. 1.

Insertion of the FRed cassette does not compromise CSF1R expression or macrophage differentiation

The *Csf1r* knockout on the C57BL/6 background is severely compromised, and few homozygotes survive to weaning (21). By contrast, CSF1R-FRed mice were healthy and fertile, and there was no apparent effect on postnatal growth or any overt phenotype in homozygotes. We first confirmed that the FRed reporter was expressed in macrophages and their progenitors and correlated with CSF1R expression. Fig. 2 compares expression of the reporter and CSF1R (CD115) in BM cells from adult WT, heterozygous, and homozygous CSF1R-FRed mice. In fresh BM, FRed expression was restricted to CD115^{+} cells (Fig. 2A) with the exception of a minor population of hematopoietic progenitors analyzed further below. In homozygotes, FRed was increased proportionate to gene dose as expected, but CD115 expression was unaffected (Fig. 2B). To confirm that the FRed insertion did not impact CSF1R function, we cultured BM from WT, heterozygous, and homozygous CSF1R-FRed mice in CSF1 to generate BM-derived macrophages (BMDM). The yield of BMDM was unaffected by the insertion. The FRed reporter was expressed homogeneously in BMDM from heterozygous CSF1R-FRed mice and around 2-fold higher in the homozygotes (Fig. 2C). Unless otherwise stated, all analysis in this study was carried out on CSF1R-FRed heterozygotes, but for some applications a homozygote might have greater utility.

Previous studies reported that *Csf1r* mRNA was first detectable in early mouse myeloid precursors on which surface CSF1R was not detectable (53). CSF1R is expressed on the surface of committed macrophage-DC and monocyte progenitors (25). The question of CSF1R expression by progenitors is key to the issue of whether CSF1 is instructive or selective in lineage commitment. It has been suggested that CSF1 instructs lineage fate in hematopoietic stem cells (HSC) by inducing the key transcriptional regulator PU.1 (54, 55). This proposal is difficult to reconcile with the fact that *Csf1r* promoter activity is stringently dependent upon PU.1 (15) and with analysis of progenitors by single cell RNA sequencing (56), which associated *Csf1r* mRNA with committed progenitors. CSF1R-FRed provides a unique marker to address this question. Aside from stem cell and committed progenitors, BM contains monocytes and multiple distinct resident macrophage populations (45). Lineage-negative BM progenitor subpopulations were analyzed as previously described based on expression of CD48, CD150, and CD117 (cKIT). The results of flow cytometry analysis of isolated BM cells are summarized in Fig. 3. Consistent with *Csf1r* mRNA expression data (53, 56), CSF1R-FRed expression was not detected in HSC or multipotent progenitors and present only within a small subset of hematopoietic progenitor cells (Lin^{-}CD48^{+}) and Lin^{-}KIT^{+}SCA1^{-} committed progenitors (Fig. 3A). Committed progenitors (common lymphoid progenitor, common myeloid progenitor [CMP], granulocyte-macrophage progenitor [GMP] and megakaryocyte-erythroid progenitor [MEP]) were further separated based on surface markers according to the hierarchical

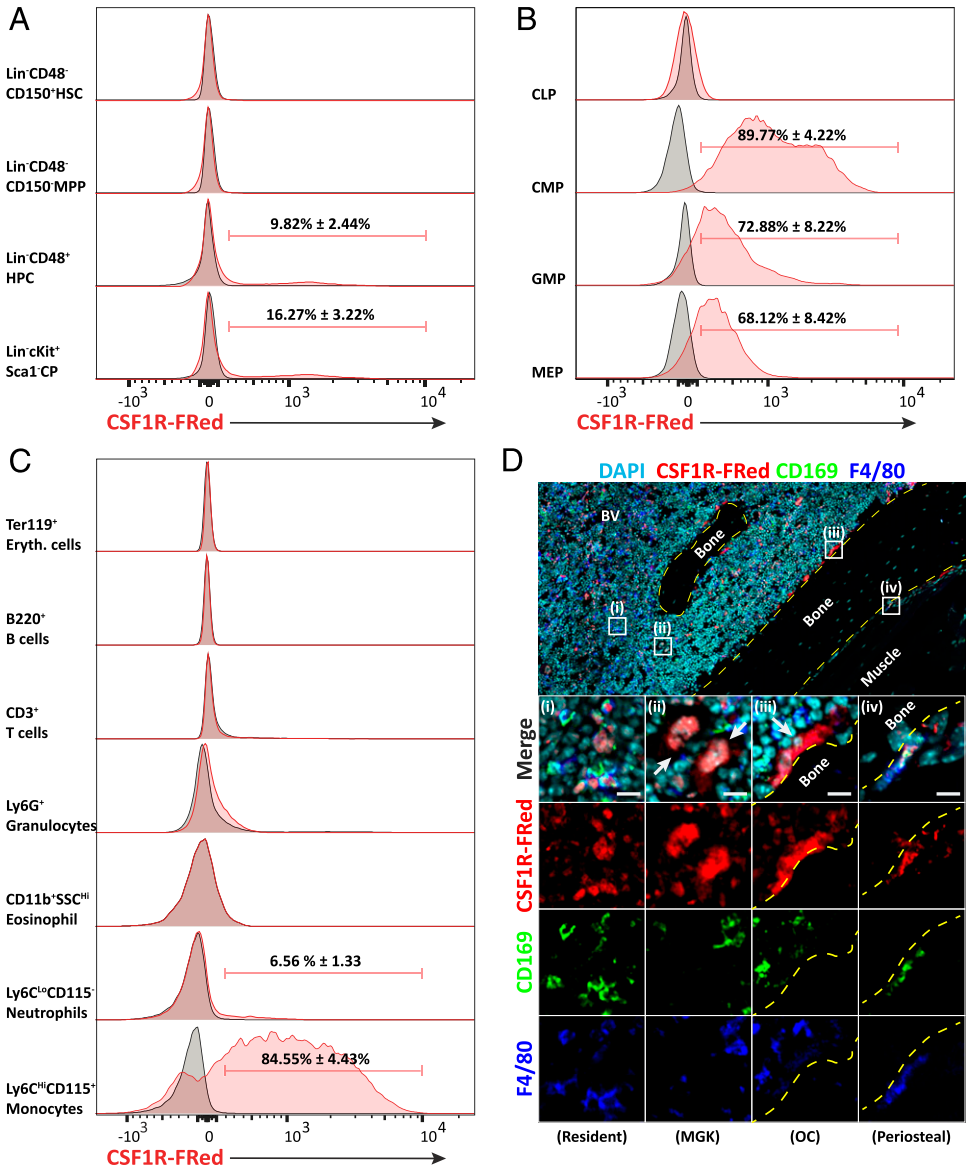

FIGURE 3. Expression of CSF1R-FRed in BM. Femoral BM cells were harvested from adult WT and CSF1R-FRed$^{+/-}$ mice and analyzed by flow cytometry using the markers indicated and gating strategies shown in Supplemental Fig. 5. (**A**) Defined stem cell populations, (**B**) committed progenitors, and (**C**) the mature leukocytes. In each case, the gray profile is the nontransgenic control, and the red profile is the CSF1R-FRed mouse. The results are representative of three mice of each genotype. (**D**) Localization of CSF1R-FRed in femoral BM. Bone was fixed and decalcified as described in *Materials and Methods* and stained for each of the markers shown. CSF1R-FRed was detected using anti-RFP Ab. Specificity controls are shown in Supplemental Fig. 7. Highlighted regions (**i**)-(**iv**) in the upper panel are shown at higher magnification in the lower panels as indicated. The staining highlights expression of CSF1R-FRed in F4/80$^+$/CD169$^+$ resident macrophages within hematopoietic islands and on the periosteal surface and in megakaryocytes (MGK) and F4/80$^-$/CD169$^-$ osteoclasts (OC). Scale bar, 20 μm.

model of Akashi et al. (57). No FRed expression was detected in common lymphoid progenitors (Fig. 3B). Surprisingly, although the two populations were uniformly positive, the CSF1R-FRed signal was considerably higher in CMP than in GMP. Signal was also detected in MEP.

In flow cytometry analysis of lineage$^+$ cells in BM suspensions, CSF1R-FRed was restricted to Ly6C^{hi}/CD115$^+$ monocytes (Fig. 3C). By contrast to *Csf1r* reporter transgenes, granulocytes, which in previous studies expressed *Csf1r* mRNA at high levels but did not express CSF1R protein detectable by Western blot (13), were CSF1R-FRed$^-$. Similarly, B cells that also express reporter transgenes did not express CSF1R-FRed, indicating that CSF1R protein regulation is controlled by elements outside the core *Csf1r* promoter and enhancer (6).

Resident macrophage subpopulations in BM associated with hematopoietic islands, as well as osteomacs lining bone surfaces, express Siglec1 (CD169) and F4/80 (58), and bone-resorbing osteoclasts are also CSF1R dependent (8). Not all of these mature myeloid cells can be reliably isolated using BM flushing, and anatomical location is needed for accurate identification. To complement the flow cytometry, we stained sections of BM using anti-RFP Ab, CD169, and F4/80 (Fig. 3D). FRed is generally stable to normal paraformaldehyde fixation. The anti-RFP Ab was used specifically for BM because prolonged fixation of intact bone and subsequent decalcification led to a partial loss of RFP signal. However, the RFP signal in marrow can be preserved by perfusion fixation with inclusion of 0.5% glutaraldehyde as well as 4% paraformaldehyde (data not shown). CSF1R-FRed was detected in all F4/80$^+$/CD169$^+$ cells forming the center of hematopoietic islands and lining the surface of bone (osteomacs) (59) and was also detected in multinucleated osteoclasts, which are F4/80$^-$. We (unpublished) and others (60) have noted that *Csf1r* reporter transgenes are also expressed by megakaryocytes and their CD41$^+$ progenitors in adult mouse BM, but expression of CSF1R protein has not been reported. The sections of BM also indicated expression of CSF1R-FRed in the majority of megakaryocytes in situ.

Mouse peripheral blood contains two populations of blood monocytes, distinguished by the level of expression of Ly6C. This is a differentiation series dependent upon CSF1R signaling. Both populations clearly express *Csf1r* mRNA and bind anti-CD115 (23, 61), albeit at relatively low levels by comparison with resident tissue macrophages (3). The Ly6C^{lo} population had somewhat higher expression of the *Csf1r*-EGFP transgene (23), but the

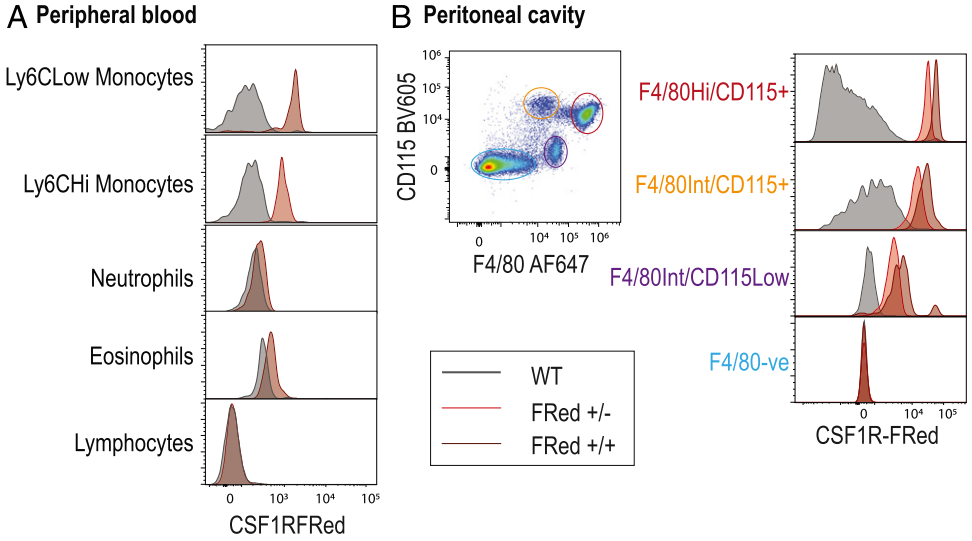

FIGURE 4. CSF1R-FRed expression in peripheral blood and peritoneal cavity leukocytes. (**A**) Peripheral blood leukocytes were isolated from WT and CSF1R-FRed$^{+/-}$ mice and analyzed by flow cytometry using gating strategies shown in Supplemental Fig. 6. Red histograms show expression in the CSF1R-FRed mice compared with WT mice (gray histograms). (**B**). Peritoneal lavage cells were isolated from WT, CSF1R-FRed$^{+/-}$, and CSF1R-FRed$^{+/+}$ and separated into four populations based on F4/80 and CD115 expression as shown. Note the increased expression in FRed$^{+/+}$ mice.

two populations were not distinguished by *Csf1r*-mApple (6). Fig. 4A shows the profile of expression of CSF1R-FRed in blood leukocytes. As observed in BM, there was no detectable expression of the FRed reporter in lymphocytes or granulocytes, whereas both monocyte populations were clearly positive with expression marginally higher in the Ly6C^{lo} population.

In the peritoneal cavity, the major F4/80^{Hi}/CD115^{+} and minor F4/80^{Int}/CD115^{+} macrophage populations expressed similar levels of FRed, whereas lower FRed expression was observed in F4/80^{Int}/CD115$^{Low/-}$ cells (Fig. 4B). The resident peritoneal macrophage population is very sensitive to anti-CSF1R treatment (23) and was selectively depleted in a *Csf1r* hypomorphic mutant mouse (5). However, as in BM, homozygosity for the CSF1R-FRed allele did not affect peritoneal macrophage abundance or labeling with F4/80/CD115, and the reporter expression was ~2-fold higher in homozygotes compared with heterozygotes (Fig. 4B).

Mononuclear phagocyte populations of lymphoid tissues

The spleen contains multiple resident macrophage and DC populations in the red pulp, the marginal zone (MZ), T cell areas, and B cell areas (62). There is also a population of undifferentiated monocytes that can be recruited to inflammatory sites (63). LN likewise contain multiple functional MPS subpopulations in the subcapsular sinus, medullary sinus, medullary cords, T cell areas, and germinal centers (64, 65). Many of these populations lack expression of surface markers such as F4/80 and are susceptible to fragmentation during tissue disaggregation (64). Fig. 5 shows colocalization of myeloid (CD169, CD68, F4/80) and lymphoid (B220, CD3) markers in sections of spleen (Fig. 5A–C) and LN (Fig. 5E, 5F). In the spleen, there was a complete overlap with F4/80 in the red pulp. In the MZ, CD169^{+} metallophils expressed CSF1R-FRed, as did a separate stellate population of F4/80^{-} macrophages, the outer MZ macrophages (66). Expression was excluded from B220 and CD3-positive lymphocytes. Multilineage flow cytometry analysis of disaggregated spleen cells confirmed the expression of CSF1R-FRed in Ly6C^{hi} monocytes and exclusion from non-MPS populations (Fig. 5D). Isolated CD11c^{hi}/F4/80^{lo} presumptive cDC were positive but heterogeneous for detectable CSF1R-FRed; consistent with detection of cells with varying levels of the reporter among the stellate interdigitating cells within the T cell areas of spleen (Fig. 5B). The CSF1R-FRed^{lo} cells within T cell areas were positive for CD68 (Fig. 5B).

Like MZ metallophils in the spleen, the majority of subcapsular sinus macrophages in LN express CD169 and lack F4/80 (65), although there is also an F4/80^{+} population on the LN surface (67). Subcapsular sinus macrophages depend upon CSF1 produced locally (65). There was almost complete overlap between CSF1R-FRed and CD169 in the subcapsular region, whereas F4/80 was detected on only a subset of cells. CSF1R-FRed was detected in the dense population of F4/80^{hi}/CD169^{+} macrophages that populate the medullary sinuses (67) and was also detectable on the network of F4/80^{-}/CD169^{-} interdigitating cells (68) found throughout T cell areas of the LN. These may include the population of T zone macrophages described by Baratin et al. (69) as well as cDC. In spleen and LN there were few positive cells in B cell areas, and there was no apparent reactivity in the so-called tingible-body macrophages.

The intestinal wall contains multiple abundant MPS subpopulations, notably the CD169^{hi} populations surrounding the crypts. All of the lamina propria populations are acutely depleted by anti-CSF1R Ab, with consequent impacts on epithelial differentiation (70). Supplemental Fig. 1 shows CSF1R-FRed expression in the small intestine. Expression was coincident with F4/80 in the stellate macrophage populations of the lamina propria, but expression of FRed also provided a unique marker for the abundant CSF1-dependent phagocyte population underlying the dome epithelium of the Peyer patch, which lacks expression of markers such as F4/80, CD169, CD206, and CD64 (71).

CSF1R-FRed expression in known and novel resident tissue MPS cells

Csf1r-EGFP and *Csf1r*-mApple reporter transgenes identified an extensive network of presumptive resident macrophages in every organ in the body (6, 7). Fig. 6 shows representative confocal images of multiple tissues from the adult CSF1R-FRed mouse highlighting the dense network of stellate interstitial cells. Direct whole mount imaging of fresh tissues without fixation highlights the full extent of this network of MPS cells. CSF1R-FRed provides improved visualization of less-studied macrophage populations, including the dense populations of macrophages in skeletal and smooth muscle, and those of the uterus and cervix, stomach, adrenal gland, Islets of Langerhans, ovary, pancreas, brown fat, and thymus.

As a multicopy transgene, the *Csf1r*-EGFP reporter is considerably brighter than CSF1R-FRed. As discussed in the introduction, it has the disadvantage of expression in granulocytes and B cells, but it still has significant utility for live imaging. To determine the overlap between the two reporters, we crossed the

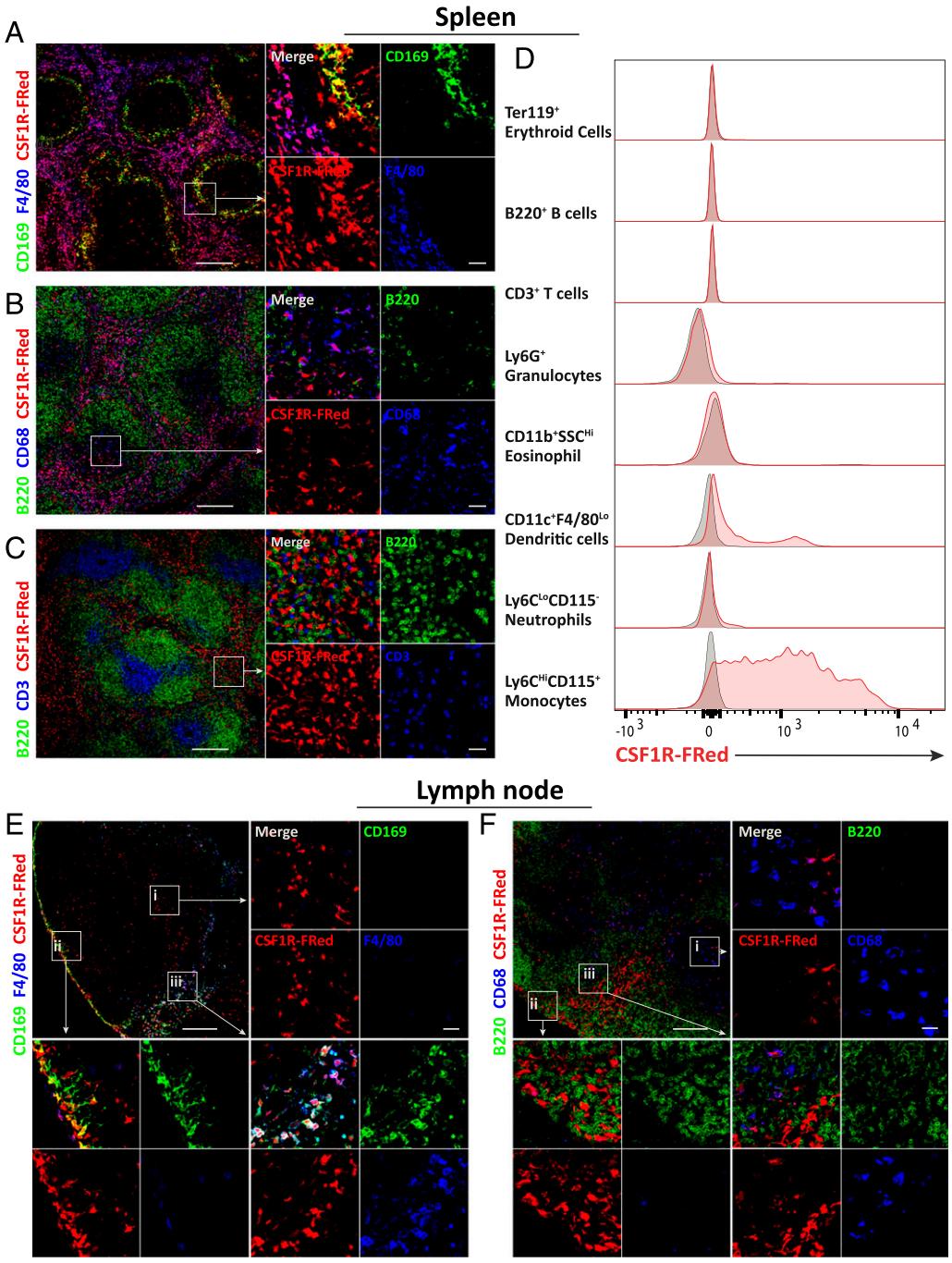

FIGURE 5. CSF1R-FRed expression in spleen and LN. Spleens and inguinal LNs were harvested from adult WT and CSF1R-FRed$^{+/-}$ mice and fixed and sectioned as described in *Materials and Methods*. Part of the spleen was disaggregated for flow cytometry analysis. In sections, CSF1R-FRed was detected by direct imaging in combination with the markers indicated. (**A**) The expression of CSF1R-FRed in F4/80^{+} red pulp macrophages, F4/80^{-}, CD169^{+} MZ metallophils, and F4/80^{-}/CD169^{-} MZ macrophages (also see insets). Scale bar, 200 μm. (**B**) CSF1R-FRed^{+} cells within T cell areas (excluded B220) and the overlap with CD68. Scale bar, 200 μm. (**C**) Exclusion of CSF1R-FRed from CD3^{+} T cells and B220^{+} B cells in the red pulp but the potential for interactions among the three cell types (also see insets). Scale bar, 200 μm. (**D**) Representative profiles for WT (gray histograms) and CSF1R-FRed (red histograms) spleen cells separated based on the gating strategy in Supplemental Fig. 6. (**E**) CSF1R-FRed expression in CD169^{-}/F4/80^{-} interdigitating cells in T cell areas [inset (**Ei**)], CD169^{+}/F4/80^{-} subcapsular sinus macrophages [inset (**Eii**)], and CD169^{+}/F4/80^{+} medullary sinus macrophages in the LN [inset (**Eiii**)]. Scale bar, 20 μm. Colocalization in (**F**) with B220 and CD68 further highlights interdigitating cells in T cell areas [inset (**Fi**)] and intimate interaction with B cells in the medullary cords/sinuses [insets (**Fii**) and (**Fiii**)]. Scale bar, 20 μm.

CSF1R-FRed and *Csf1r*-EGFP lines. Recent studies have identified populations of CSF1R-dependent mononuclear phagocytes underlying the liver capsule and distinct from Kupffer cells (72, 73). These cells were implicated in defense against infiltration of the liver by pathogens in the peritoneal cavity. The liver capsular macrophages were detected using the expression of a *Cd207*-EGFP reporter transgene, a marker shared with Langerhans cells of the skin. The *Cd207*-EGFP reporter transgene was not detected in the capsule of other organs, leading to the conclusion that the presence of these cells is unique to the liver (73). A confocal Z series inwards from the liver surface confirmed the detection of these cells with *Csf1r*-EGFP and CSF1R-FRed and the transition

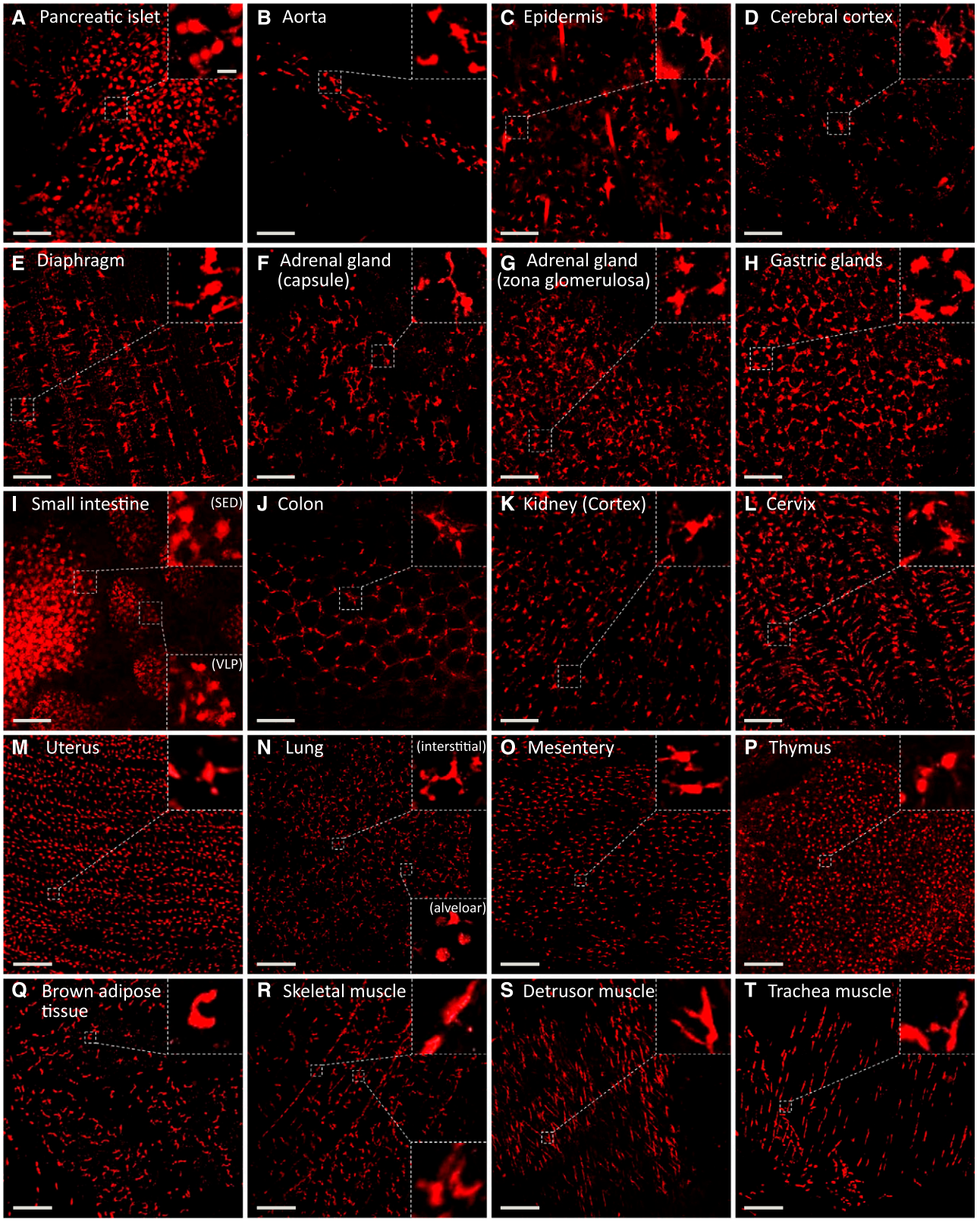

FIGURE 6. (**A**–**T**) Imaging of macrophages in adult organs using CSF1R-FRed. Tissues were removed from adult CSF1R-FRed$^{+/-}$ mice and placed on ice in PBS. They were imaged directly within 2–3 h using an Olympus FV3000 microscope. Images show maximum intensity projections of the tissues indicated. Many of these tissues can also be visualized as Z series in Supplemental Videos 1–17. Scale bar, 100 μm.

from the subcapsular population to classical Kupffer cells (Supplemental Video 1).

A similar series for the brain cortex (Supplemental Video 2) highlights the abundant macrophage population of the dura mater and leptomeninges (74) and the transition to the underlying network of microglia. Luo et al. (75) reported the expression of *Csf1r* in neurons and claimed that systemic CSF1 treatment could ameliorate neuronal injury by direct signaling. Contrary to that

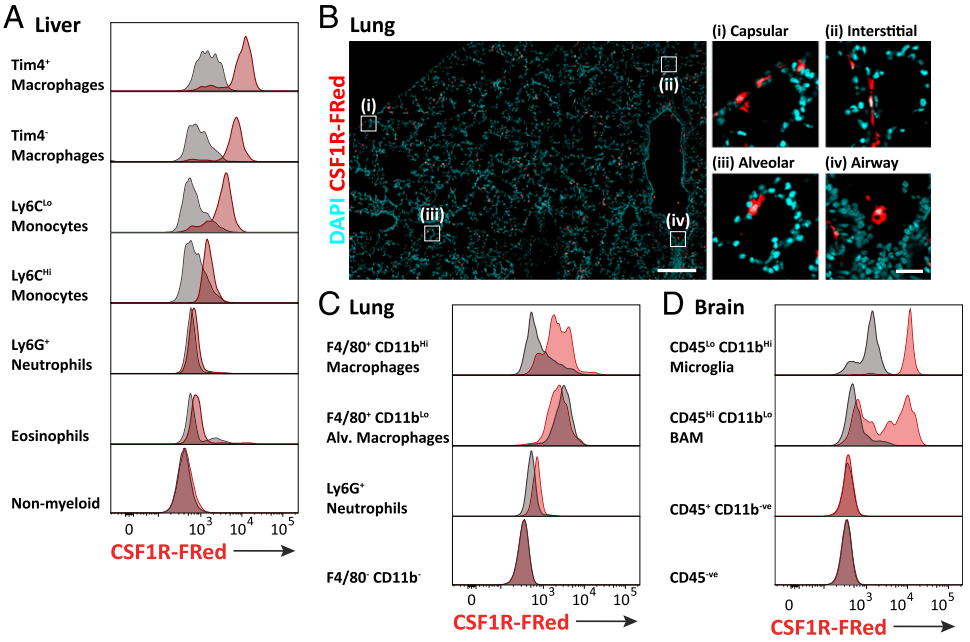

FIGURE 7. Expression of CSF1R-FRed in liver, lung, and brain. Leukocytes were isolated from liver (**A**), lung (**C**), and brain (**D**) following tissue disaggregation as described in *Materials and Methods* and analyzed by flow cytometry for expression of the indicated markers. The gating strategies are shown in Supplemental Fig. 6. Note in (C) that alveolar macrophages have high levels of autofluorescence, which may obscure a FRed signal. To confirm expression in lung macrophage populations, (**B**) shows localization of CSF1R-FRed in unfixed lung sections. (**i**–**iv**) Insets highlight four CSF1R-FRed^{+} populations distinguished by location and morphology. Scale bars, 200 μm in main image and 20 μm in magnified image.

report, expression of the *Csf1r*-EGFP transgene is entirely restricted to microglia and brain-associated macrophages (20, 21). However, there is the formal possibility that the *Csf1r*-EGFP reporter construct lacks elements required for expression in neurons. Supplemental Fig. 2 shows that CSF1R-FRed expression was not detectable in neurons in the dentate gyrus of the hippocampus, even in CSF1R-FRed$^{+/+}$ mice with additional amplification provided by anti-RFP Ab.

The population of surface-associated or subcapsular macrophages was not restricted to the liver. The CSF1R reporter transgenes enable confocal imaging of the surface of every major organ of the body and reveal that surface-associated macrophages are a universal feature. The relative density and stellate morphology of surface-associated macrophages is remarkably consistent. In each case, a confocal Z series from the outer surface reveals transitions in morphology and location of the underlying resident tissue macrophages. Supplemental Videos 3–17 show Z series for the two reporters through the depth of a selection of organs, including the liver, lung, heart, brain, kidney, large intestine, periosteum, skeletal muscle, abdominal wall, epididymis, vas deferens adrenal, and bladder. There was a complete overlap between the GFP and FRed reporters. Separate static and merged images of each reporter in selected tissues are shown in Supplemental Fig. 3. In each case, the Z series highlights the way in which the polarity of the macrophage spreading changes in various layers to align with the orientation of surface connective tissues/serosa/mesothelial layers, underlying muscle fibers, connective tissues, and other structures.

To confirm the macrophage-restricted expression and utility for macrophage isolation, we used conventional disaggregation procedures to isolate cells from liver, lung, and brain and characterized the populations by flow cytometry (Fig. 7). In each organ, expression was excluded from both lymphocytes and CD45^{-} populations. In the liver, there is a complete overlap between CSF1R-FRed and F4/80 labeling of sinusoidal Kupffer cells (Supplemental Fig. 4). In isolated cells, the expression of CSF1R-FRed increased progressively from monocytes to mature TIM4^{+} Kupffer cells (Fig. 7A) consistent with gene expression analysis of this progression (76). In the lung, CSF1R-FRed was expressed by interstitial monocyte and macrophage populations (Fig. 7B, 7C). The expression in alveolar macrophages (F4/80^{int}/CD11b^{lo}) analyzed by flow cytometry is obscured by very high autofluorescence and the relatively low *Csf1r* mRNA (2). Autofluorescence is less of an issue in confocal imaging. We confirmed expression in bronchial and alveolar populations and in interstitial and subcapsular cells in situ (Fig. 7B). In the brain, CSF1R-FRed was detected in both microglia (CD45^{lo}/CD11b^{hi}) and brain-associated macrophages (CD45^{hi}/CD11b^{lo}) (Fig. 7D) and, consistent with Supplemental Fig. 2, was absent from CD45^{-} cells.

Discussion

We have described the generation and characterization of a CSF1R reporter mouse line. The *Csf1r* promoter region including the conserved FIRE element has been used to drive reporter transgenes and direct expression of constitutive and tamoxifen-inducible cre-recombinase and the macrophage Fas-induced apoptosis (MaFIA) transgene for conditional macrophage ablation (4). These applications have been compromised by the expression of *Csf1r* mRNA and/or *Csf1r* promoter-driven transgenes in other hematopoietic cells and the potential for ectopic expression in multicopy transgenes. Many other myeloid promoters and target loci (e.g., *Adgre1*, *Ccr2*, *Cd68*, *Cd169*, *Cd11c*, *Cd11b*, *Clec9a*, *Cx3cr1*, *Flt3*, *LysM*, *Ms4a3*, *Tmem119*, *Zbtb46*) have been used to drive myeloid-restricted expression of reporters, cre-recombinase, diphtheria toxin receptor (DTR), or other genes of interest. However, none of these alternatives is expressed universally and exclusively at the mRNA or protein level in all cells of the MPS (3). The CSF1R-FRed reporter mouse overcomes the confounding issues, providing a specific and robust MPS reporter for a large range of technical applications.

One future application of the *Csf1r-FRed* allele lies in study of the transcriptional regulation of the *Csf1r* locus. Deletion of the FIRE enhancer within intron two of *Csf1r* led to the loss of expression in monocytes and various tissue macrophages, including microglia, whereas other macrophage populations were unaffected. These impacts could only be assessed in homozygous mutant mice by the loss of the affected cell population (5). Several candidate enhancers other than FIRE have been identified in the *Csf1r* locus (5). Their role may be assessed by targeted deletion in

CSF1R-FRed mice and analysis of expression of the mutated allele on a heterozygous *Csf1r* WT background.

From a purely technical viewpoint, the outcome establishes the feasibility of inserting any desired expression cassette (e.g., other reporters, gene of interest, Cre, DTR) into the mouse *Csf1r* locus to achieve universal MPS-restricted expression without disrupting expression or function of CSF1R protein. We have bred the *Csf1r-FRed* allele to homozygosity, and there is no detectable impact on viability, growth, monocyte-macrophage abundance, surface markers (e.g., F4/80), or the expression of CSF1R on the cell surface (Fig. 3). Accordingly, for many applications, CSF1R-FRed can be maintained as a homozygous line and conveniently crossed to other reporters (as exemplified by the cross to the *Csf1r*-EGFP reporter). We note also that the FRed reporter is expressed in macrophages of homozygotes at around twice the level in heterozygotes (Figs. 3, 5). It is not self-evident that this would be the case because the expression of *Csf1r* mRNA is regulated by CSF1R signals and the expression from the two alleles might be coordinated (77). The reciprocal observation is that in heterozygous *Csf1r* knockout mice and rats, there is no dosage compensation, and both *Csf1r* mRNA and protein are reduced by 50% on monocytes and macrophages (2). It appears, therefore, that *Csf1r* alleles are regulated independently of each other.

The expression of CSF1R-FRed in BM accords with other evidence that *Csf1r* mRNA is absent from HSC and induced during lineage commitment downstream of expression of lineage-specific transcription factors (53, 56). The large majority of lineage-negative, CD115$^+$ cells in BM are in cell cycle (25). The lack of detectable CSF1R-FRed in HSC is not compatible with the proposal that CSF1 acts directly on HSC to instruct myeloid lineage commitment via induction of PU.1 (55). These studies relied on detection of *Csf1r* mRNA in HSC by quantitative RT-PCR and did not detect the CSF1R protein. The reported effects of CSF1 on PU.1 expression in isolated HSC were small, and significant numbers of PU.1-expressing cells arose spontaneously even in the absence of added CSF1. Accordingly, we favor a selective model of CSF1 action in which PU.1 lies upstream of *Csf1r*. Interestingly, although CSF1 administration can induce a substantial monocytosis, CSF1R signaling is not absolutely required for monocyte production. Anti-CSF1R Ab treatment of mice depleted tissue macrophages but had no effect on the blood monocyte count (23, 24), and mutation of the *Csf1r* FIRE enhancer ablated *Csf1r* expression in BM and blood monocytes without impacting abundance or phenotype of these cells (5). CSF1R-FRed was more highly expressed and somewhat heterogeneous within CMP compared with GMP as defined using CD32 as a marker (57). Several recent studies question the hierarchical model of myelopoiesis in which CMP give rise to GMP. They indicate that CD115^{hi} monocyte-DC progenitors (32) and committed monocyte progenitors (25) may both reside within the CMP fraction of BM (Ref. 78 and references therein). Conversely, Kwok et al. (79) dissected the GMP populations to reveal a predominance of CD115^{lo} committed neutrophil progenitors consistent with low expression of CSF1R-FRed in this fraction (Fig. 3B). There is a previous report of low expression of CSF1R, detected by FACS using anti-CD115, in circulating mouse granulocytes (80), but the expression of CSF1R-FRed in Ly6G$^+$ granulocytes was barely detectable (Fig. 4A). That conclusion is supported by the lack of detectable binding of labeled CSF1 to granulocytes in both mice and rats (6, 8, 81). In terms of our core objective in generating this line, the relative expression of CSF1R-FRed is more than adequate to unequivocally distinguish MPS cells from granulocytes and B cells. There is no evidence of a nonredundant function of CSF1R in granulocytopoiesis based on *CSF1R* mutations in mouse, rat, or human (2).

The immunolocalization of the FRed reporter in the BM revealed the expression of CSF1R in megakaryocytes (Fig. 3D). Expression profiling of mouse megakaryocyte differentiation in vitro supported expression of *Csf1r* mRNA, which declined in the most mature population (82). This conclusion is consistent with detection of CSF1R-FRed in the MEP population (Fig. 3B). The functional importance of CSF1/CSF1R in megakaryocyte biology is unknown. In humans, *CSF1R* is commonly deleted in 5q-syndrome, which is associated with thrombocytopenia (83), but homozygous mutation in *CSF1R* in rats or humans had no impact on platelet count (81, 84). Conversely, in humans, mice, and pigs, CSF1 administration causes a rapid fall in platelet count (85–88). In mice, this drop resolved with a significant overshoot, even with continued CSF1 treatment, associated with alterations in megakaryocyte ploidy (86). CSF1-induced thrombocytopenia was attributed to reduced circulating half-life; but the possibility that CSF1 might also drive the rebound was not excluded.

cDC in spleen, LN, and also in Peyer patches form a dense network of interdigitating cells within the T cell areas (68). The *Csf1r*-EGFP transgene was expressed by interdigitating cells in spleen and LN T cells areas and by CD11c^{hi} DC isolated from spleen and LN, and surface CD115 was detected on a subset of these cells (34). The level of *Csf1r* mRNA also distinguishes CD8$^+$ (cDC1) and CD8$^-$ DC isolated from spleen (BioGPS.org, Immgen.org) and cDC1 (XCR1$^+$, CD103$^+$) from cDC2 (CD11b$^+$) in multiple large RNA sequencing datasets (3), with relatively higher expression by cDC2. CSF1R-FRed was detected at varying levels in isolated CD11c^{hi} spleen DC and may provide a subset marker (Fig. 5). Given the extensive ramification of the interdigitating cells within T cell areas, it is likely that they are underrepresented in populations obtained by enzymic disaggregation. The expression of CSF1R-FRed is consistent with evidence that cDC in lymphoid tissues are dependent upon CSF1R signals (34, 35).

Other macrophage populations in spleen and LN that have not been isolated by tissue disaggregation include those of the MZ and subcapsular sinus. We colocalized CSF1R-FRed with F4/80 (which is excluded from the MZ and T cell areas) and CD169 (expressed by both MZ and subcapsular sinus macrophages) (Fig. 5). CSF1R-FRed was detected in red pulp (F4/80^{hi}) and MZ (CD169$^+$/F4/80$^-$) macrophages. Unexpectedly, CSF1R-FRed was undetectable in the large tingible-body macrophages in germinal centers, which do express *Csf1r*-EGFP but are CSF1R independent (23). These cells express CD68 and MERTK, which is required for apoptotic B cell uptake (89). Unlike follicular DC, they are BM derived (90), but they also lack other myeloid markers, including IBA1 and F4/80 (91, 92).

Flow cytometry analysis and imaging of multiple tissues confirms that, like *Csf1r* mRNA, CSF1R-FRed is expressed throughout the MPS. By contrast to previous reports (75, 93, 94) we found no evidence of CSF1R protein expression in brain neuronal cells or epithelial cell populations in intestine or kidney. Accordingly, the numerous pleotropic impacts of *CSF1R* mutations and kinase inhibitors in humans and experimental animals can be attributed entirely to indirect consequences of MPS cell deficiency (reviewed in Ref. 2).

In nonlymphoid tissues, there was a complete overlap of CSF1R-FRed with *Csf1r*-EGFP, supporting the utility of this transgenic marker (Supplemental Fig. 3). Not surprisingly, as a multicopy transgene, the signal from *Csf1r*-EGFP is generally much brighter than CSF1R-FRed, but the signal intensities are not perfectly correlated. There are cells in several of the tissues analyzed that

appear more red than green, perhaps reflecting the fact that the transgenic reporter does not contain all the *Csf1r* regulatory elements (5). Both transgenes viewed in unfixed fresh tissues highlight the full extent of the MPS network in every tissue. *Csf1r* mRNA is readily detected in total mRNA from all the organs shown at levels around 10% of that detected in BMDM (95), so the density of these cells is not surprising. Within tissues, CSF1R-FRed$^+$/*Csf1r*-EGFP$^+$ cells appear spread on surfaces such as epithelial and endothelial basement membranes and muscle and connective tissue fibers. Both reporters highlighted the so-called tenophages recently identified in tendon (96). The localization of CSF1R-FRed/*Csf1r*-EGFP confirmed the existence of surface-associated macrophages underlying the serosa and spread in the plane of the capsule in every major organ. They include the heterogeneous population of macrophages associated with the dura mater of the brain, previously characterized using CX3R1, MHC class II, CD169, IBA1, and CD11c (74) and recently isolated and profiled as a distinct population from microglia (97). Conversely, the dense subcapsular macrophage population of the lung was not recognized or characterized in studies of interstitial macrophage heterogeneity (98). These surface-associated macrophage populations present in every organ were identified in the original studies of the localization of the F4/80 Ag (reviewed in Ref. 16) but are not readily visualized in cross-section. It remains to be determined whether they have organ-specific innate immune or homeostatic functions or share phenotypes with the cells identified in the liver (72, 73).

One location where the abundance of resident macrophages has been underappreciated is muscle. The macrophages of the smooth muscle of the intestinal muscularis have been attributed functions in interactions with enteric neurons and the control of peristalsis and gut motility (99). Whole mount imaging of these cells with the CSF1R-FRed and *Csf1r*-EGFP reporter reveals their abundance within the myenteric plexus, the way in which they spread along the muscle fibers, and change polarity between the longitudinal and circular muscle layers. The same transitions are evident in layers of smooth muscle in large intestine, abdominal wall, diaphragm, uterus/cervix, vas deferens, and bladder as well as cardiac muscle (Fig. 6E, 6I, 6L, 6M, Supplemental Videos 4, 8, 9, 12, 17). By contrast, there is very limited literature on macrophages in skeletal muscle, where CSF1R-FRed-positive cells are at least as abundant as in smooth muscle, with the same regular spacing along the muscle fibers (see Fig. 6R–T, Supplemental Video 7). Previous studies using immunohistochemical markers (CD11b, F4/80, CD45) identified abundant resident macrophage-like populations in the epimysium and perimysium (the external muscle envelope) but rarely detected positive cells in the endomysium (the thin layer between muscle fibers) (100, 101). This may partly be a reflection of their extensive spreading and that detection is further compromised by fixation (which causes the macrophages to contract) and sectioning (which tears them from the muscle fibers). However, it may also be that the markers are not expressed. Standard methods of tissue disaggregation yield very few macrophage-like cells from undamaged muscle. A recent study reported the isolation and characterization of mouse skeletal muscle macrophages (101) but is unclear whether the isolated cells are representative of the large resident population. The resident tissue macrophages in muscle are well positioned to interact with satellite cells and the neuromuscular junctions and contribute similar regulatory, homeostatic, and remodeling functions to resident macrophages identified in the heart and vascular smooth muscle (102–104) that were also readily visualized with CSF1R-FRed and *Csf1r*-EGFP.

The locations occupied by tissue macrophages have been referred to as niches or territories. The concepts differ depending on whether the precise location is physically defined (a niche) or macrophages define their own territory by mutual repulsion (1, 105). The regular spacing in every location (Fig. 6) supports the territory concept. The two concepts are compatible if a niche exists on a macroscopic scale (e.g., a particular surface) and macrophages determine their density within the niche. Almost universal expression of semaphorins and their receptors (known regulators of cell motility) (3) in isolated tissue macrophages from all organs provides at least one possible mechanism for communication between resident macrophages.

In summary, we have produced a mouse transgenic line that provides a specific and ubiquitous marker for MPS cells and highlights their distribution in every organ of the body. Given the abundance of these cells, it is not surprising that their depletion in CSF1R-deficient mice, rats, and humans has profound impacts on postnatal growth and development (2).

Disclosures

The authors have no financial conflicts of interest.

References

1. Hume, D. A., K. M. Irvine, and C. Pridans. 2019. The mononuclear phagocyte system: the relationship between monocytes and macrophages. *Trends Immunol.* 40: 98–112.
2. Hume, D. A., M. Caruso, M. Ferrari-Cestari, K. M. Summers, C. Pridans, and K. M. Irvine. 2020. Phenotypic impacts of CSF1R deficiencies in humans and model organisms. *J. Leukoc. Biol.* 107: 205–219.
3. Summers, K. M., S. J. Bush, and D. A. Hume. Transcriptional network analysis of transcriptomic diversity in resident tissue macrophages and dendritic cells in the mouse mononuclear phagocyte system. *PLoS Biol.* DOI: 10.1371/journal.pbio.3000859.
4. Rojo, R., C. Pridans, D. Langlais, and D. A. Hume. 2017. Transcriptional mechanisms that control expression of the macrophage colony-stimulating factor receptor locus. *Clin. Sci. (Lond.)* 131: 2161–2182.
5. Rojo, R., A. Raper, D. D. Ozdemir, L. Lefevre, K. Grabert, E. Wollscheid-Lengeling, B. Bradford, M. Caruso, I. Gazova, A. Sánchez, et al. 2019. Deletion of a Csf1r enhancer selectively impacts CSF1R expression and development of tissue macrophage populations. *Nat. Commun.* 10: 3215.
6. Hawley, C. A., R. Rojo, A. Raper, K. A. Sauter, Z. M. Lisowski, K. Grabert, C. C. Bain, G. M. Davis, P. A. Louwe, M. C. Ostrowski, et al. 2018. *Csf1r*-mApple transgene expression and ligand binding in vivo reveal dynamics of CSF1R expression within the mononuclear phagocyte system. *J. Immunol.* 200: 2209–2223.
7. Sasmono, R. T., D. Oceandy, J. W. Pollard, W. Tong, P. Pavli, B. J. Wainwright, M. C. Ostrowski, S. R. Himes, and D. A. Hume. 2003. A macrophage colony-stimulating factor receptor-green fluorescent protein transgene is expressed throughout the mononuclear phagocyte system of the mouse. *Blood* 101: 1155–1163.
8. Irvine, K. M., M. Caruso, M. F. Cestari, G. M. Davis, S. Keshvari, A. Sehgal, C. Pridans, and D. A. Hume. 2020. Analysis of the impact of CSF-1 administration in adult rats using a novel Csf1r-mApple reporter gene. *J. Leukoc. Biol.* 107: 221–235.
9. Balic, A., C. Chintoan-Uta, P. Vohra, K. M. Sutton, R. L. Cassady-Cain, T. Hu, D. S. Donaldson, M. P. Stevens, N. A. Mabbott, D. A. Hume, et al. 2019. Antigen sampling *CSF1R*-expressing epithelial cells are the functional equivalents of mammalian M cells in the avian follicle-associated epithelium. *Front. Immunol.* 10: 2495.
10. Balic, A., C. Garcia-Morales, L. Vervelde, H. Gilhooley, A. Sherman, V. Garceau, M. W. Gutowska, D. W. Burt, P. Kaiser, D. A. Hume, and H. M. Sang. 2014. Visualisation of chicken macrophages using transgenic reporter genes: insights into the development of the avian macrophage lineage. *Development* 141: 3255–3265.
11. Pridans, C., G. M. Davis, K. A. Sauter, Z. M. Lisowski, Y. Corripio-Miyar, A. Raper, L. Lefevre, R. Young, M. E. McCulloch, S. Lillico, et al. 2016. A Csf1r-EGFP transgene provides a novel marker for monocyte subsets in sheep. *J. Immunol.* 197: 2297–2305.
12. Hu, T., Z. Wu, S. J. Bush, L. Freem, L. Vervelde, K. M. Summers, D. A. Hume, A. Balic, and P. Kaiser. 2019. Characterization of subpopulations of chicken mononuclear phagocytes that express TIM4 and CSF1R. *J. Immunol.* 202: 1186–1199.
13. Sasmono, R. T., A. Ehrnsperger, S. L. Cronau, T. Ravasi, R. Kandane, M. J. Hickey, A. D. Cook, S. R. Himes, J. A. Hamilton, and D. A. Hume. 2007. Mouse neutrophilic granulocytes express mRNA encoding the macrophage colony-stimulating factor receptor (CSF-1R) as well as many other macrophage-specific transcripts and can transdifferentiate into macrophages in vitro in response to CSF-1. *J. Leukoc. Biol.* 82: 111–123.

14. Ross, I. L., T. L. Dunn, X. Yue, S. Roy, C. J. Barnett, and D. A. Hume. 1994. Comparison of the expression and function of the transcription factor PU.1 (Spi-1 proto-oncogene) between murine macrophages and B lymphocytes. *Oncogene* 9: 121–132.
15. Ross, I. L., X. Yue, M. C. Ostrowski, and D. A. Hume. 1998. Interaction between PU.1 and another Ets family transcription factor promotes macrophage-specific Basal transcription initiation. *J. Biol. Chem.* 273: 6662–6669.
16. Hume, D. A. 2008. Differentiation and heterogeneity in the mononuclear phagocyte system. *Mucosal Immunol.* 1: 432–441.
17. Chitu, V., Ş. Gokhan, S. Nandi, M. F. Mehler, and E. R. Stanley. 2016. Emerging roles for CSF-1 receptor and its ligands in the nervous system. *Trends Neurosci.* 39: 378–393.
18. Chitu, V., and E. R. Stanley. 2017. Regulation of embryonic and postnatal development by the CSF-1 receptor. *Curr. Top. Dev. Biol.* 123: 229–275.
19. Nandi, S., S. Gokhan, X. M. Dai, S. Wei, G. Enikolopov, H. Lin, M. F. Mehler, and E. R. Stanley. 2012. The CSF-1 receptor ligands IL-34 and CSF-1 exhibit distinct developmental brain expression patterns and regulate neural progenitor cell maintenance and maturation. *Dev. Biol.* 367: 100–113.
20. De Lucia, C., A. Rinchon, A. Olmos-Alonso, K. Riecken, B. Fehse, D. Boche, V. H. Perry, and D. Gomez-Nicola. 2016. Microglia regulate hippocampal neurogenesis during chronic neurodegeneration. *Brain Behav. Immun.* 55: 179–190.
21. Erblich, B., L. Zhu, A. M. Etgen, K. Dobrenis, and J. W. Pollard. 2011. Absence of colony stimulation factor-1 receptor results in loss of microglia, disrupted brain development and olfactory deficits. *PLoS One* 6: e26317.
22. Bennett, F. C., M. L. Bennett, F. Yaqoob, S. B. Mulinyawe, G. A. Grant, M. Hayden Gephart, E. D. Plowey, and B. A. Barres. 2018. A combination of ontogeny and CNS environment establishes microglial identity. *Neuron* 98: 1170–1183.e8.
23. MacDonald, K. P., J. S. Palmer, S. Cronau, E. Seppanen, S. Olver, N. C. Raffelt, R. Kuns, A. R. Pettit, A. Clouston, B. Wainwright, et al. 2010. An antibody against the colony-stimulating factor 1 receptor depletes the resident subset of monocytes and tissue- and tumor-associated macrophages but does not inhibit inflammation. *Blood* 116: 3955–3963.
24. Sudo, T., S. Nishikawa, M. Ogawa, H. Kataoka, N. Ohno, A. Izawa, S. Hayashi, and S. Nishikawa. 1995. Functional hierarchy of c-kit and c-fms in intramarrow production of CFU-M. *Oncogene* 11: 2469–2476.
25. Hettinger, J., D. M. Richards, J. Hansson, M. M. Barra, A. C. Joschko, J. Krijgsveld, and M. Feuerer. 2013. Origin of monocytes and macrophages in a committed progenitor. *Nat. Immunol.* 14: 821–830.
26. Stanley, E. R., and V. Chitu. 2014. CSF-1 receptor signaling in myeloid cells. *Cold Spring Harb. Perspect. Biol.* 6: a021857.
27. Sester, D. P., S. J. Beasley, M. J. Sweet, L. F. Fowles, S. L. Cronau, K. J. Stacey, and D. A. Hume. 1999. Bacterial/CpG DNA down-modulates colony stimulating factor-1 receptor surface expression on murine bone marrow-derived macrophages with concomitant growth arrest and factor-independent survival. *J. Immunol.* 163: 6541–6550.
28. Sester, D. P., A. Trieu, K. Brion, K. Schroder, T. Ravasi, J. A. Robinson, R. C. McDonald, V. Ripoll, C. A. Wells, H. Suzuki, et al. 2005. LPS regulates a set of genes in primary murine macrophages by antagonising CSF-1 action. *Immunobiology* 210: 97–107.
29. Anderson, D. A., III, and K. M. Murphy. 2019. Models of dendritic cell development correlate ontogeny with function. *Adv. Immunol.* 143: 99–119.
30. Guilliams, M., F. Ginhoux, C. Jakubzick, S. H. Naik, N. Onai, B. U. Schraml, E. Segura, R. Tussiwand, and S. Yona. 2014. Dendritic cells, monocytes and macrophages: a unified nomenclature based on ontogeny. *Nat. Rev. Immunol.* 14: 571–578.
31. Merad, M., P. Sathe, J. Helft, J. Miller, and A. Mortha. 2013. The dendritic cell lineage: ontogeny and function of dendritic cells and their subsets in the steady state and the inflamed setting. *Annu. Rev. Immunol.* 31: 563–604.
32. Auffray, C., D. K. Fogg, E. Narni-Mancinelli, B. Senechal, C. Trouillet, N. Saederup, J. Leemput, K. Bigot, L. Campisi, M. Abitbol, et al. 2009. CX3CR1+ CD115+ CD135+ common macrophage/DC precursors and the role of CX3CR1 in their response to inflammation. *J. Exp. Med.* 206: 595–606.
33. Gautier, E. L., T. Shay, J. Miller, M. Greter, C. Jakubzick, S. Ivanov, J. Helft, A. Chow, K. G. Elpek, S. Gordonov, et al; Immunological Genome Consortium. 2012. Gene-expression profiles and transcriptional regulatory pathways that underlie the identity and diversity of mouse tissue macrophages. *Nat. Immunol.* 13: 1118–1128.
34. MacDonald, K. P., V. Rowe, H. M. Bofinger, R. Thomas, T. Sasmono, D. A. Hume, and G. R. Hill. 2005. The colony-stimulating factor 1 receptor is expressed on dendritic cells during differentiation and regulates their expansion. *J. Immunol.* 175: 1399–1405.
35. Durai, V., P. Bagadia, C. G. Briseño, D. J. Theisen, A. Iwata, J. T. Davidson, IV, M. Gargaro, D. H. Fremont, T. L. Murphy, and K. M. Murphy. 2018. Altered compensatory cytokine signaling underlies the discrepancy between *Flt3*$^{-/-}$ and *Flt3l*$^{-/-}$ mice. *J. Exp. Med.* 215: 1417–1435.
36. Ginhoux, F., K. Liu, J. Helft, M. Bogunovic, M. Greter, D. Hashimoto, J. Price, N. Yin, J. Bromberg, S. A. Lira, et al. 2009. The origin and development of nonlymphoid tissue CD103+ DCs. *J. Exp. Med.* 206: 3115–3130.
37. Ginhoux, F., F. Tacke, V. Angeli, M. Bogunovic, M. Loubeau, X. M. Dai, E. R. Stanley, G. J. Randolph, and M. Merad. 2006. Langerhans cells arise from monocytes in vivo. *Nat. Immunol.* 7: 265–273.
38. Jung, S., J. Aliberti, P. Graemmel, M. J. Sunshine, G. W. Kreutzberg, A. Sher, and D. R. Littman. 2000. Analysis of fractalkine receptor CX(3)CR1 function by targeted deletion and green fluorescent protein reporter gene insertion. *Mol. Cell. Biol.* 20: 4106–4114.
39. Saederup, N., A. E. Cardona, K. Croft, M. Mizutani, A. C. Cotleur, C. L. Tsou, R. M. Ransohoff, and I. F. Charo. 2010. Selective chemokine receptor usage by central nervous system myeloid cells in CCR2-red fluorescent protein knock-in mice. *PLoS One* 5: e13693.
40. Liu, Z., Y. Gu, S. Chakarov, C. Bleriot, I. Kwok, X. Chen, A. Shin, W. Huang, R. J. Dress, C. A. Dutertre, et al. 2019. Fate mapping via ms4a3-expression history traces monocyte-derived cells. *Cell* 178: 1509–1525.e19.
41. Ruan, C., L. Sun, A. Kroshilina, L. Beckers, P. De Jager, E. M. Bradshaw, S. A. Hasson, G. Yang, and W. Elyaman. 2020. A novel Tmem119-tdTomato reporter mouse model for studying microglia in the central nervous system. *Brain Behav. Immun.* 83: 180–191.
42. Masuda, T., L. Amann, R. Sankowski, O. Staszewski, M. Lenz, P. D Errico, N. Snaidero, M. J. Costa Jordão, C. Böttcher, K. Kierdorf, et al. 2020. Novel Hexb-based tools for studying microglia in the CNS. *Nat. Immunol.* 21: 802–815.
43. Quadros, R. M., H. Miura, D. W. Harms, H. Akatsuka, T. Sato, T. Aida, R. Redder, G. P. Richardson, Y. Inagaki, D. Sakai, et al. 2017. Easi-CRISPR: a robust method for one-step generation of mice carrying conditional and insertion alleles using long ssDNA donors and CRISPR ribonucleoproteins. *Genome Biol.* 18: 92.
44. Demayo, J. L., J. Wang, D. Liang, R. Zhang, and F. J. Demayo. 2012. Genetically engineered mice by pronuclear DNA microinjection. *Curr. Protoc. Mouse Biol.* 2: 245–262.
45. Kaur, S., L. J. Raggatt, S. M. Millard, A. C. Wu, L. Batoon, R. N. Jacobsen, I. G. Winkler, K. P. MacDonald, A. C. Perkins, D. A. Hume, et al. 2018. Self-repopulating recipient bone marrow resident macrophages promote long-term hematopoietic stem cell engraftment. *Blood* 132: 735–749.
46. Gow, D. J., V. Garceau, C. Pridans, A. G. Gow, K. E. Simpson, D. Gunn-Moore, and D. A. Hume. 2013. Cloning and expression of feline colony stimulating factor receptor (CSF-1R) and analysis of the species specificity of stimulation by colony stimulating factor-1 (CSF-1) and interleukin-34 (IL-34). *Cytokine* 61: 630–638.
47. Pridans, C., K. A. Sauter, K. Baer, H. Kissel, and D. A. Hume. 2013. CSF1R mutations in hereditary diffuse leukoencephalopathy with spheroids are loss of function. *Sci. Rep.* 3: 3013.
48. Shemiakina, I. I., G. V. Ermakova, P. J. Cranfill, M. A. Baird, R. A. Evans, E. A. Souslova, D. B. Staroverov, A. Y. Gorokhovatsky, E. V. Putintseva, T. V. Gorodnicheva, et al. 2012. A monomeric red fluorescent protein with low cytotoxicity. *Nat. Commun.* 3: 1204.
49. Ryan, M. D., A. M. King, and G. P. Thomas. 1991. Cleavage of foot-and-mouth disease virus polyprotein is mediated by residues located within a 19 amino acid sequence. *J. Gen. Virol.* 72: 2727–2732.
50. Luke, G. A., and M. D. Ryan. 2018. Using the 2A protein coexpression system: multicistronic 2A vectors expressing gene(s) of interest and reporter proteins. *Methods Mol. Biol.* 1755: 31–48.
51. Lange, A., M. Gegg, I. Burtscher, D. Bengel, E. Kremmer, and H. Lickert. 2012. Fltp(T2AiCre): a new knock-in mouse line for conditional gene targeting in distinct mono- and multiciliated tissues. *Differentiation* 83: S105–S113.
52. Szymczak, A. L., C. J. Workman, Y. Wang, K. M. Vignali, S. Dilioglou, E. F. Vanin, and D. A. Vignali. 2004. Correction of multi-gene deficiency in vivo using a single 'self-cleaving' 2A peptide-based retroviral vector. *Nat. Biotechnol.* 22: 589–594.
53. Tagoh, H., R. Himes, D. Clarke, P. J. Leenen, A. D. Riggs, D. Hume, and C. Bonifer. 2002. Transcription factor complex formation and chromatin fine structure alterations at the murine c-fms (CSF-1 receptor) locus during maturation of myeloid precursor cells. *Genes Dev.* 16: 1721–1737.
54. Kandalla, P. K., S. Sarrazin, K. Molawi, C. Berruyer, D. Redelberger, A. Favel, C. Bordi, S. de Bentzmann, and M. H. Sieweke. 2016. M-CSF improves protection against bacterial and fungal infections after hematopoietic stem/progenitor cell transplantation. *J. Exp. Med.* 213: 2269–2279.
55. Mossadegh-Keller, N., S. Sarrazin, P. K. Kandalla, L. Espinosa, E. R. Stanley, S. L. Nutt, J. Moore, and M. H. Sieweke. 2013. M-CSF instructs myeloid lineage fate in single haematopoietic stem cells. *Nature* 497: 239–243.
56. Giladi, A., F. Paul, Y. Herzog, Y. Lubling, A. Weiner, I. Yofe, D. Jaitin, N. Cabezas-Wallscheid, R. Dress, F. Ginhoux, et al. 2018. Single-cell characterization of haematopoietic progenitors and their trajectories in homeostasis and perturbed haematopoiesis. *Nat. Cell Biol.* 20: 836–846.
57. Akashi, K., D. Traver, T. Miyamoto, and I. L. Weissman. 2000. A clonogenic common myeloid progenitor that gives rise to all myeloid lineages. *Nature* 404: 193–197.
58. Kaur, S., L. J. Raggatt, L. Batoon, D. A. Hume, J. P. Levesque, and A. R. Pettit. 2017. Role of bone marrow macrophages in controlling homeostasis and repair in bone and bone marrow niches. *Semin. Cell Dev. Biol.* 61: 12–21.
59. Chang, M. K., L. J. Raggatt, K. A. Alexander, J. S. Kuliwaba, N. L. Fazzalari, K. Schroder, E. R. Maylin, V. M. Ripoll, D. A. Hume, and A. R. Pettit. 2008. Osteal tissue macrophages are intercalated throughout human and mouse bone lining tissues and regulate osteoblast function in vitro and in vivo. *J. Immunol.* 181: 1232–1244.
60. Cortegano, I., N. Serrano, C. Ruiz, M. Rodríguez, C. Prado, M. Alía, A. Hidalgo, E. Cano, B. de Andrés, and M. L. Gaspar. 2019. CD45 expression discriminates waves of embryonic megakaryocytes in the mouse. *Haematologica* 104: 1853–1865.
61. Mildner, A., J. Schonheit, A. Giladi, E. David, D. Lara-Astiaso, E. Lorenzo-Vivas, F. Paul, L. Chappell-Maor, J. Priller, A. Leutz, et al. 2017. Genomic characterization of murine monocytes reveals C/EBPβ transcription factor dependence of Ly6C - cells. *Immunity* 46: 849–862.e7.

62. Gordon, S., and P. R. Taylor. 2005. Monocyte and macrophage heterogeneity. *Nat. Rev. Immunol.* 5: 953–964.
63. Swirski, F. K., M. Nahrendorf, M. Etzrodt, M. Wildgruber, V. Cortez-Retamozo, P. Panizzi, J. L. Figueiredo, R. H. Kohler, A. Chudnovskiy, P. Waterman, et al. 2009. Identification of splenic reservoir monocytes and their deployment to inflammatory sites. *Science* 325: 612–616.
64. Gray, E. E., and J. G. Cyster. 2012. Lymph node macrophages. *J. Innate Immun.* 4: 424–436.
65. Mondor, I., M. Baratin, M. Lagueyrie, L. Saro, S. Henri, R. Gentek, D. Suerinck, W. Kastenmuller, J. X. Jiang, and M. Bajenoff. 2019. Lymphatic endothelial cells are essential components of the subcapsular sinus macrophage niche. *Immunity* 50: 1453–1466.e4.
66. Gordon, S., A. Plüddemann, and S. Mukhopadhyay. 2014. Sinusoidal immunity: macrophages at the lymphohematopoietic interface. *Cold Spring Harb. Perspect. Biol.* 7: a016378.
67. Hume, D. A., A. P. Robinson, G. G. MacPherson, and S. Gordon. 1983. The mononuclear phagocyte system of the mouse defined by immunohistochemical localization of antigen F4/80. Relationship between macrophages, Langerhans cells, reticular cells, and dendritic cells in lymphoid and hematopoietic organs. *J. Exp. Med.* 158: 1522–1536.
68. Dudziak, D., A. O. Kamphorst, G. F. Heidkamp, V. R. Buchholz, C. Trumpfheller, S. Yamazaki, C. Cheong, K. Liu, H. W. Lee, C. G. Park, et al. 2007. Differential antigen processing by dendritic cell subsets in vivo. *Science* 315: 107–111.
69. Baratin, M., L. Simon, A. Jorquera, C. Ghigo, D. Dembele, J. Nowak, R. Gentek, S. Wienert, F. Klauschen, B. Malissen, et al. 2017. T cell zone resident macrophages silently dispose of apoptotic cells in the lymph node. *Immunity* 47: 349–362.e5.
70. Sehgal, A., D. S. Donaldson, C. Pridans, K. A. Sauter, D. A. Hume, and N. A. Mabbott. 2018. The role of CSF1R-dependent macrophages in control of the intestinal stem-cell niche. *Nat. Commun.* 9: 1272.
71. Wagner, C., J. Bonnardel, C. Da Silva, L. Martens, J. P. Gorvel, and H. Lelouard. 2018. Some news from the unknown soldier, the Peyer's patch macrophage. *Cell. Immunol.* 330: 159–167.
72. David, B. A., R. M. Rezende, M. M. Antunes, M. M. Santos, M. A. Freitas Lopes, A. B. Diniz, R. V. Sousa Pereira, S. C. Marchesi, D. M. Alvarenga, B. N. Nakagaki, et al. 2016. Combination of mass cytometry and imaging analysis reveals origin, location, and functional repopulation of liver myeloid cells in mice. *Gastroenterology* 151: 1176–1191.
73. Sierro, F., M. Evrard, S. Rizzetto, M. Melino, A. J. Mitchell, M. Florido, L. Beattie, S. B. Walters, S. S. Tay, B. Lu, et al. 2017. A liver capsular network of monocyte-derived macrophages restricts hepatic dissemination of intraperitoneal bacteria by neutrophil recruitment. *Immunity* 47: 374–388.e6.
74. Chinnery, H. R., M. J. Ruitenberg, and P. G. McMenamin. 2010. Novel characterization of monocyte-derived cell populations in the meninges and choroid plexus and their rates of replenishment in bone marrow chimeric mice. *J. Neuropathol. Exp. Neurol.* 69: 896–909.
75. Luo, J., F. Elwood, M. Britschgi, S. Villeda, H. Zhang, Z. Ding, L. Zhu, H. Alabsi, R. Getachew, R. Narasimhan, et al. 2013. Colony-stimulating factor 1 receptor (CSF1R) signaling in injured neurons facilitates protection and survival. *J. Exp. Med.* 210: 157–172.
76. Sakai, M., T. D. Troutman, J. S. Seidman, Z. Ouyang, N. J. Spann, Y. Abe, K. M. Ego, C. M. Bruni, Z. Deng, J. C. M. Schlachetzki, et al. 2019. Liver-derived signals sequentially reprogram myeloid enhancers to initiate and maintain kupffer cell identity. *Immunity* 51: 655–670.e8.
77. Yue, X., P. Favot, T. L. Dunn, A. I. Cassady, and D. A. Hume. 1993. Expression of mRNA encoding the macrophage colony-stimulating factor receptor (c-fms) is controlled by a constitutive promoter and tissue-specific transcription elongation. *Mol. Cell. Biol.* 13: 3191–3201.
78. Yanez, A., S. G. Coetzee, A. Olsson, D. E. Muench, B. P. Berman, D. J. Hazelett, N. Salomonis, H. L. Grimes, and H. S. Goodridge. 2017. Granulocyte-monocyte progenitors and monocyte-dendritic cell progenitors independently produce functionally distinct monocytes. *Immunity* 47: 890–902.e4.
79. Kwok, I., E. Becht, Y. Xia, M. Ng, Y. C. Teh, L. Tan, M. Evrard, J. L. Y. Li, H. T. N. Tran, Y. Tan, et al. 2020. Combinatorial single-cell analyses of granulocyte-monocyte progenitor heterogeneity reveals an early uni-potent neutrophil progenitor. *Immunity* 53: 303–318.e5.
80. Jakubzick, C., M. Bogunovic, A. J. Bonito, E. L. Kuan, M. Merad, and G. J. Randolph. 2008. Lymph-migrating, tissue-derived dendritic cells are minor constituents within steady-state lymph nodes. *J. Exp. Med.* 205: 2839–2850.
81. Pridans, C., A. Raper, G. M. Davis, J. Alves, K. A. Sauter, L. Lefevre, T. Regan, S. Meek, L. Sutherland, A. J. Thomson, et al. 2018. Pleiotropic impacts of macrophage and microglial deficiency on development in rats with targeted mutation of the *Csf1r* locus. *J. Immunol.* 201: 2683–2699.
82. Chen, Z., M. Hu, and R. A. Shivdasani. 2007. Expression analysis of primary mouse megakaryocyte differentiation and its application in identifying stage-specific molecular markers and a novel transcriptional target of NF-E2. *Blood* 109: 1451–1459.
83. Lehmann, S., J. O'Kelly, S. Raynaud, S. E. Funk, E. H. Sage, and H. P. Koeffler. 2007. Common deleted genes in the 5q- syndrome: thrombocytopenia and reduced erythroid colony formation in SPARC null mice. *Leukemia* 21: 1931–1936.
84. Guo, L., D. R. Bertola, A. Takanohashi, A. Saito, Y. Segawa, T. Yokota, S. Ishibashi, Y. Nishida, G. L. Yamamoto, J. F. D. S. Franco, et al. 2019. Bi-allelic CSF1R mutations cause skeletal dysplasia of dysosteosclerosis-pyle disease spectrum and degenerative encephalopathy with brain malformation. *Am. J. Hum. Genet.* 104: 925–935.
85. Gow, D. J., K. A. Sauter, C. Pridans, L. Moffat, A. Sehgal, B. M. Stutchfield, S. Raza, P. M. Beard, Y. T. Tsai, G. Bainbridge, et al. 2014. Characterisation of a novel Fc conjugate of macrophage colony-stimulating factor. *Mol. Ther.* 22: 1580–1592.
86. Baker, G. R., and J. Levin. 1998. Transient thrombocytopenia produced by administration of macrophage colony-stimulating factor: investigations of the mechanism. *Blood* 91: 89–99.
87. Jakubowski, A. A., D. F. Bajorin, M. A. Templeton, P. B. Chapman, B. V. Cody, H. Thaler, Y. Tao, D. A. Filippa, L. Williams, M. L. Sherman, et al. 1996. Phase I study of continuous-infusion recombinant macrophage colony-stimulating factor in patients with metastatic melanoma. *Clin. Cancer Res.* 2: 295–302.
88. Sauter, K. A., L. A. Waddell, Z. M. Lisowski, R. Young, L. Lefevre, G. M. Davis, S. M. Clohisey, M. McCulloch, E. Magowan, N. A. Mabbott, et al. 2016. Macrophage colony-stimulating factor (CSF1) controls monocyte production and maturation and the steady-state size of the liver in pigs. *Am. J. Physiol. Gastrointest. Liver Physiol.* 311: G533–G547.
89. Rahman, Z. S., W. H. Shao, T. N. Khan, Y. Zhen, and P. L. Cohen. 2010. Impaired apoptotic cell clearance in the germinal center by Mer-deficient tingible body macrophages leads to enhanced antibody-forming cell and germinal center responses. *J. Immunol.* 185: 5859–5868.
90. Kranich, J., N. J. Krautler, E. Heinen, M. Polymenidou, C. Bridel, A. Schildknecht, C. Huber, M. H. Kosco-Vilbois, R. Zinkernagel, G. Miele, and A. Aguzzi. 2008. Follicular dendritic cells control engulfment of apoptotic bodies by secreting Mfge8. *J. Exp. Med.* 205: 1293–1302.
91. Köhler, C. 2007. Allograft inflammatory factor-1/Ionized calcium-binding adapter molecule 1 is specifically expressed by most subpopulations of macrophages and spermatids in testis. *Cell Tissue Res.* 330: 291–302.
92. Kraal, G., M. Rep, and M. Janse. 1987. Macrophages in T and B cell compartments and other tissue macrophages recognized by monoclonal antibody MOMA-2. An immunohistochemical study. *Scand. J. Immunol.* 26: 653–661.
93. Akcora, D., D. Huynh, S. Lightowler, M. Germann, S. Robine, J. R. de May, J. W. Pollard, E. R. Stanley, J. Malaterre, and R. G. Ramsay. 2013. The CSF-1 receptor fashions the intestinal stem cell niche. *Stem Cell Res. (Amst.)* 10: 203–212.
94. Menke, J., Y. Iwata, W. A. Rabacal, R. Basu, Y. G. Yeung, B. D. Humphreys, T. Wada, A. Schwarting, E. R. Stanley, and V. R. Kelley. 2009. CSF-1 signals directly to renal tubular epithelial cells to mediate repair in mice. *J. Clin. Invest.* 119: 2330–2342.
95. Summers, K. M., and D. A. Hume. 2017. Identification of the macrophage-specific promoter signature in FANTOM5 mouse embryo developmental time course data. *J. Leukoc. Biol.* 102: 1081–1092.
96. Lehner, C., G. Spitzer, R. Gehwolf, A. Wagner, N. Weissenbacher, C. Deininger, K. Emmanuel, F. Wichlas, H. Tempfer, and A. Traweger. 2019. Tenophages: a novel macrophage-like tendon cell population expressing CX3CL1 and CX3CR1. *Dis. Model. Mech.* 12: dmm041384.
97. Van Hove, H., L. Martens, I. Scheyltjens, K. De Vlaminck, A. R. Pombo Antunes, S. De Prijck, N. Vandamme, S. De Schepper, G. Van Isterdael, C. L. Scott, et al. 2019. A single-cell atlas of mouse brain macrophages reveals unique transcriptional identities shaped by ontogeny and tissue environment. *Nat. Neurosci.* 22: 1021–1035.
98. Schyns, J., Q. Bai, C. Ruscitti, C. Radermecker, S. De Schepper, S. Chakarov, F. Farnir, D. Pirottin, F. Ginhoux, G. Boeckxstaens, et al. 2019. Non-classical tissue monocytes and two functionally distinct populations of interstitial macrophages populate the mouse lung. *Nat. Commun.* 10: 3964.
99. De Schepper, S., N. Stakenborg, G. Matteoli, S. Verheijden, and G. E. Boeckxstaens. 2018. Muscularis macrophages: key players in intestinal homeostasis and disease. *Cell. Immunol.* 330: 142–150.
100. Brigitte, M., C. Schilte, A. Plonquet, Y. Baba-Amer, A. Henri, C. Charlier, S. Tajbakhsh, M. Albert, R. K. Gherardi, and F. Chrétien. 2010. Muscle resident macrophages control the immune cell reaction in a mouse model of notexin-induced myoinjury. *Arthritis Rheum.* 62: 268–279.
101. Wang, X., A. A. Sathe, G. R. Smith, F. Ruf-Zamojski, V. Nair, K. J. Lavine, C. Xing, S. C. Sealfon, and L. Zhou. 2020. Heterogeneous origins and functions of mouse skeletal muscle-resident macrophages. *Proc. Natl. Acad. Sci. USA* 117: 20729–20740.
102. Bajpai, G., C. Schneider, N. Wong, A. Bredemeyer, M. Hulsmans, M. Nahrendorf, S. Epelman, D. Kreisel, Y. Liu, A. Itoh, et al. 2018. The human heart contains distinct macrophage subsets with divergent origins and functions. *Nat. Med.* 24: 1234–1245.
103. Hulsmans, M., S. Clauss, L. Xiao, A. D. Aguirre, K. R. King, A. Hanley, W. J. Hucker, E. M. Wulfers, G. Seemann, G. Courties, et al. 2017. Macrophages facilitate electrical conduction in the heart. *Cell* 169: 510–522.e20.
104. Lim, H. Y., S. Y. Lim, C. K. Tan, C. H. Thiam, C. C. Goh, D. Carbajo, S. H. S. Chew, P. See, S. Chakarov, X. N. Wang, et al. 2018. Hyaluronan receptor LYVE-1-expressing macrophages maintain arterial tone through hyaluronan-mediated regulation of smooth muscle cell collagen. [Published erratum appears in 2018 *Immunity* 49: 1191.] *Immunity* 49: 326–341.e7.
105. Guilliams, M., G. R. Thierry, J. Bonnardel, and M. Bajenoff. 2020. Establishment and maintenance of the macrophage niche. *Immunity* 52: 434–451.